JOURNAL OF VIROLOGY, May 2005, p. 6005–6022 Vol. 79, No. 10
0022-538X/05/$08.00+0 doi:10.1128/JVI.79.10.6005–6022.2005

Targeting Human Glioblastoma Cells: Comparison of Nine Viruses with Oncolytic Potential

Guido Wollmann,[1] Peter Tattersall,[2] and Anthony N. van den Pol[1]*

Department of Neurosurgery[1] and Laboratory Medicine and Genetics,[2] Yale University School of Medicine, New Haven, CT 06520

Received 3 September 2004/Accepted 4 January 2005

Brain tumors classified as glioblastomas have proven refractory to treatment and generally result in death within a year of diagnosis. We used seven in vitro tests and one in vivo trial to compare the efficacy of nine different viruses for targeting human glioblastoma. Green fluorescent protein (GFP)-expressing vesicular stomatitis (VSV), Sindbis virus, pseudorabies virus (PRV), adeno-associated virus (AAV), and minute virus of mice i-strain (MVMi) and MVMp all infected glioblastoma cells. Mouse and human cytomegalovirus, and simian virus 40 showed only low levels of infection or GFP expression. VSV and Sindbis virus showed strong cytolytic actions and high rates of replication and spread, leading to an elimination of glioblastoma. PRV and both MVM strains generated more modest lytic effects and replication capacity. VSV showed a similar oncolytic profile on U-87 MG and M059J glioblastoma. In contrast, Sindbis virus showed strong preference for U-87 MG, whereas MVMi and MVMp preferred M059J. Sindbis virus and both MVM strains showed highly tumor-selective actions in glioblastoma plus fibroblast coculture. VSV and Sindbis virus were serially passaged on glioblastoma cells; we isolated a variant, VSV-rp30, that had increased selectivity and lytic capacity in glioblastoma cells. VSV and Sindbis virus were very effective at replicating, spreading within, and selectively killing human glioblastoma in an in vivo mouse model, whereas PRV and AAV remained at the injection site with minimal spread. Together, these data suggest that four (VSV, Sindbis virus, MVMi, and MVMp) of the nine viruses studied merit further analysis for potential therapeutic actions on glioblastoma.

Malignant glioblastomas are the most common primary brain tumors and have withstood all attempts for curative treatment. Each year, about 17,000 new malignant brain tumor cases are diagnosed in the United States and more than 13,000 deaths are attributed to these neoplasms (2, 30). With current treatment protocols, the median survival in humans is less than a year after diagnosis, with very few long-term survivors (64).

A variety of viral vectors, including retroviruses, herpesviruses, and adenoviruses, have been tested for oncolytic potential against glioblastoma (11, 18, 45, 46, 61). We are, however, not aware of any study that directly compares the antitumor profiles of unrelated viruses. Here, we approach this question by evaluating parameters indicative for the outcome of viral infection. Nine DNA and RNA viruses were compared for their tropism for glioblastoma cells, their effect on tumor cell proliferation, and the induction of cell death. We further explored whether glioblastoma cells are permissive for virus replication and whether newly released viral progeny generate a self-amplification of the oncolytic effect. To accommodate the heterogeneity of glioblastoma, multiple glioma cell lines with distinct geno- and phenotypes were compared. In addition, we evaluated whether viral infection and replication is selective for glioblastoma compared to non-glioblastoma control cells. Finally, we examined whether the in vitro viral replication results correlate with intratumoral spread in an in vivo solid tumor model.

The selection of candidate viruses for the present study was based on several criteria. No virus with a biohazard rating greater than BL-2 was used. All viruses used could potentially be modified genetically with procedures at hand to add to or alter the viral genome. To this end, we used recombinant viruses that expressed green fluorescent protein (GFP) for two reasons: to track infections in live tumor cells and to use viruses in which a gene has already been added and in which the reporter gene could be replaced with toxic genes, potentially controlled by regulatable promoters. We focused predominantly on replication-competent viruses that could potentially infect a tumor cell and produce progeny leading to further infection and the death of neighboring tumor cells. The experiments here are designed to determine which viruses may have an inherent affinity for human glioblastoma cells. Later experiments could then use the top candidates for additional genetic or laboratory manipulation.

Vesicular stomatitis virus (VSV) is an enveloped, negative-stranded RNA rhabdovirus with a single nonsegmented genome of 11.2 kb that contains only five protein-encoding genes (N, P, M, G, and L). VSV generates an infection in a wide variety of species, including cattle, horse, and swine. Infection in humans is rare and usually asymptomatic with sporadic cases of mild flu-like symptoms (47). Recent studies have shown that VSV can exert an oncolytic profile by taking advantage of defects in the interferon system, a common feature in malignancies (5, 6, 40, 53, 54). In a previous study we found a cytolytic effect of a recombinant GFP-expressing VSV on human primary glial tumor culture (58).

Sindbis virus (SIN) is a small, enveloped, single positive-stranded RNA alphavirus with an 11.7-kb genome (19). The laboratory strain AR339 used in this study is not known to cause human disease (22). The potential use of SIN as a gene

* Corresponding author. Mailing address: Department of Neurosurgery, Yale University School of Medicine, 333 Cedar St., New Haven, CT 06520. Phone: (203) 785-5823. Fax: (203) 737-2159. E-mail: anthony.vandenpol@yale.edu.

therapy vector has been the subject of several recent studies (57, 67). Numerous aspects make this virus an interesting candidate for cancer therapy. It binds the high-affinity laminin receptor for cell entry (63) that is overexpressed in many tumor cells; it induces apoptosis in infected cells upon cell entry (25), and its blood-borne nature may be useful for systemic application.

Pseudorabies virus (PRV), an alphaherpesvirus, is a large enveloped DNA virus that does not appear to cause disease in higher primates and humans (10). The resistance of normal human cells to productive PRV infection and the absence of a preexisting immunity are favorable aspects that promote the idea of its application as a gene therapy tool. Two recent studies have raised the possibility of using PRV as a gene transfer vector or as an oncolytic agent (9, 43).

Cytomegalovirus (CMV), a betaherpesvirus, has a double-stranded 235-kb DNA genome. Viral replication is host species specific. However, mouse CMV (mCMV) can potentially act as a gene delivery vector for human cells since the mechanisms that determine the species specificity seem not to affect virus attachment and entry (36). In fact a recombinant mCMV transferred the reporter gene GFP to brain cultures and tissues from 11 species including human, confirming the feasibility of this idea (59, 60). mCMV has an enhanced affinity for astrocytes in culture, inflicting cell death 2 to 3 days after infection. Human glial cell cultures infected with mCMV, however, remained intact throughout the study and were able to express virus-delivered reporter genes (59). Human CMV (hCMV) has also been reported to have an affinity for glial cells (32). In order to investigate whether human glioma cells could be targeted by this virus, we included both human and mouse CMV in this comparative study.

Minute virus of mice (MVM), an autonomous parvovirus, is a nonenveloped, linear single-stranded DNA viruses. The natural host range of MVM is restricted to mice. Viral replication depends on host cell factors expressed during the S phase of the cell cycle, a requirement that augments, but is not entirely responsible for, the inherent oncotropism of autonomous parvoviruses (13, 34, 51). Previous studies reported successful targeting and oncolysis of human tumor cell lines (29, 49, 66). The two strains included in our study, the fibrotropic prototype MVMp and the immunosuppressive strain MVMi, differ in their capsid protein, which is critical for differences in cell targeting and outcome of infection (7, 55).

Adeno-associated virus (AAV) is a parvovirus with a nonenveloped linear single-stranded DNA that requires the coinfection of a helper virus for its own replication. AAVs have a wide host range and infect a variety of both dividing and nondividing cells. To date, AAV has not been related to any disease in humans. Wild-type AAV may also have an inherent oncoprotective action (8, 50). Recombinant AAV has been used in antiglioma studies as a vector for delivery of therapeutic genes (33, 35, 65). We used a replication-incompetent AAV2 expressing GFP in the present study for control purposes.

Simian virus 40 (SV40), a small nonenveloped polyomavirus, has a double-stranded circular DNA genome (~5 kb) encoding small and large T-antigen (early genes), and three structural proteins. Several studies have suggested the incidence of SV40 in brain tumors to be significantly higher than in nonneoplastic brain tissue (27, 62), suggesting a possible affinity for brain tumors; a causative relationship remains hypothetical. We included SV40 in our study to analyze whether an attraction to dividing neoplastic brain cells exists and whether recombinant SV40, expressing GFP in place of the viral T antigens might exhibit any kind of oncospecificity.

The purpose of the present study is to compare the characteristics of these nine viruses, seven of them replication competent, in terms of their affinity for human glioblastoma cells. Focusing on viruses that might have inherent oncolytic potential, we addressed the idea that the antineoplastic efficiency of any potential candidate depends on (i) the ability to infect and destroy tumor cells selectively, (ii) the nature of self-amplification through viral replication, and (iii) the potential to actively spread through the tumor mass. Previous studies have used other viruses in a variety of oncolytic tests. Here we compare the glioblastoma oncolytic profiles of a number of viruses that may have potential for treatment of malignant brain tumors.

MATERIALS AND METHODS

Cell lines. The human glioblastoma tumor cell lines U-87 MG and M059J were obtained from the American Type Culture Collection (Rockville, MD) and propagated in minimal essential medium supplemented with 10% fetal bovine serum and 1% sodium pyruvate (U-87 MG) or Dulbecco modified Eagle medium with 10% fetal bovine serum (M059J), respectively. Cell lines U-118 MG, A-172, and U-373 MG were kindly provided by R. Matthews (Yale University, New Haven, CT). U-118 MG and A-172 lines are commercially available at the American Type Culture Collection (Rockville, MD); U-373 can be obtained from the ECACC (Salisbury, Great Britain). The age of the cells did not exceed 15 passages. Normal human dermal fibroblasts were purchased from Cambrex (Walkersville, MD) and maintained in fibroblast basal medium supplemented with hFGF-B and insulin (Cambrex). Fibroblasts were induced to grow by changing the medium to Dulbecco modified Eagle medium with 10% fetal bovine serum until they reached full confluency and turned into contact-inhibited cells. All cells were propagated in a humidified atmosphere containing 5% CO_2 at 37°C.

Viruses. A brief description of each virus used for the experiments is given below. Details regarding construction and characteristics of recombinant viruses can be found at the indicated references.

(i) VSV. A recombinant variant of the Indiana strain of VSV containing a GFP-VSV G fusion protein as an extra gene downstream of the native VSV G protein gene, kindly provided by J. K. Rose and K. Dalton (Yale University, New Haven, CT), was used in the present study (14, 28, 58); the virus was maintained on baby hamster kidney cells (BHK-21). BHK cells were used for virus plaque assay titers.

(ii) SIN. A recombinant SIN expressing GFP was a gift from J. M. Hardwick (Johns Hopkins University, Baltimore, MD). Details regarding virus vector construction and production are found elsewhere (22). In brief, a construct consisting of a duplicated copy of the viral subgenomic promoter and a BstEII cloning site was inserted into the 3′ regulatory region of SIN genome plasmid. The cloning site can be universally used for the expression of genes of interest, in this case GFP. Virus was collected from supernatants from transfected cells, and titers were determined by plaque assay on BHK cells.

(iii) PRV. Recombinant PRV strain 152, kindly provided by L. W. Enquist (Princeton University, Princeton, NJ), was used in the present study (52). The EGFP expression cassette was cloned into a fragment containing the gG gene of PRV-Becker, which was than subjected to homologous recombination with the purified PRV-Bartha genome. The expression of EGFP was driven by the hCMV immediate-early promoter. PK15 cells were used for virus production and plaque assay.

(iv) MVM. Viral stocks for the two strains MVMi and MVMp were generated by transfecting 324K (MVMi) and A9 (MVMp) cells with pMVMi or pMVMp plasmids, respectively (17). Transfected cells were transferred to larger dishes to promote cell division required for viral replication. After 5 to 7 days, virus was collected by repeated freeze-thawing cycles of the harvested cells in TE8.7 buffer, purified by using standard sucrose gradient centrifugation, and titrated by plaque assay as described elsewhere (55).

(v) hCMV. Recombinant hCMV expressing enhanced GFP under the control of the cellular elongation factor promoter (EF1α) (26) was kindly provided by J. Vieira (University of Washington, Seattle). The gene coding for EGFP was inserted between US9 and US10 of the human CMV genome, a site that appears to tolerate alterations without affecting viral replication. GFP expression and replication capability were tested on normal human fibroblasts.

(vi) mCMV. Enhanced GFP-expressing recombinant mCMV (MC.55) was derived from the K181 strain. The expression cassette containing the GFP gene controlled by the human elongation factor 1α was inserted into the immediate-early gene (IE-2) site (59). NIH 3T3 cells were used for viral propagation and plaque assay.

(vii) AAV. The recombinant AAV2 vector was provided by K. R. Clark (Ohio State University, Columbus). GFP expression was driven by a CMV ie1 promoter. The virus was produced in a HeLa-based cell system transfected with plasmids carrying viral *rep* and *cap* genes and the ie1-CMV-GFP expression cassette flanked by the AAV-ITRs as previously described (12). Virus production was initiated upon infection with adenovirus 5. Final purification steps ensured the absence of wild-type AAV and adenovirus contamination, resulting in replication-incompetent GFP-expressing recombinant AAV2.

(viii) SV40. Recombinant SV40 was kindly provided by D. DiMaio (Yale University, New Haven, CT). The virus was produced based on a previously described SV40 vector system (38) in which the sequence for large and small T-antigen was replaced by the bovine papillomavirus (BPV) E2 gene. Here, a CMV promoter-controlled GFP expression cassette was inserted in place of the BPV sequences. For generating recombinant SV40, CMT4 cells that express large T-antigen under control of a Zn^{2+} and Cd^{2+} inducible promoter were transfected with a pucEcoSB11 plasmid containing the SV40 structural genes and the GFP expression cassette. In some control experiments, wild-type SV40 was used.

Cell culture experiments. Tumor cells were seeded in 24-well plates at a density of 20,000 cells per well in triplicate for each condition. After 12 h, the 5 to 10% confluent monolayer was washed with phosphate-buffered saline (PBS). 1 ml of serum free medium was added to each dish containing either 10^6 PFU (multiplicity of infection [MOI] = 50) or 2×10^4 PFU (MOI 1) of recombinant virus or no virus (control). After 6 h, fetal bovine serum was added to each dish to make a final concentration of 10%. After 3 days, 0.5 ml of the medium was replaced by fresh medium containing 10% serum.

(i) Cell growth kinetics. An initial cell count of 10 fields per dish was performed by placing the plates under a microscope shortly after the virus or mock infection started. For a systematic counting, fields were grouped into four central and six peripheral fields. For orientation, the center of each dish was marked. At the specified time points, counting was repeated in the same manner, thereby achieving a high match of corresponding fields.

(ii) Cytotoxicity assay. Ethidium homodimer (EthD-1; Molecular Probes, Eugene, OR) was used to label dead cells. According to the manufacturer's instructions, 20 μl of EthD-1 stock was dissolved in 10 ml of PBS (plus Ca^{2+} and Mg^{2+}). The medium was carefully removed and replaced by 250 μl of EthD-1 solution per dish. After 40 min of incubation at 37°C, the dead cells were counted based on red fluorescence of nuclei.

(iii) GFP-reported gene expression. All viruses tested with the exception of MVMi and MVMp were recombinant viruses expressing green fluorescent protein (GFP) as a reporter for cell infection. Green fluorescence was detected by using an Olympus IX71 fluorescence microscope. Counting of green cells was performed as described above with the same dishes as for cell growth analysis. Positive controls were included for every virus by infecting permissive cells (as indicated previously in the section on viruses).

(iv) Replication and viral spread. A grid pattern with 1- to 2-mm intersections was scratched with a diamond knife on poly-D-lysine coated glass coverslips (22 by 22 mm) that were placed into 35-mm petri dishes. Then, 2 ml of a cell suspension containing ca. 50,000 cells per ml was added to cover the glass. After 12 h the growth medium was replaced by serum-free medium containing 1 million PFU of the particular virus. After 6 h the dish was washed five times with fresh medium. To avoid contamination with any unincorporated virus particle, single glass pieces with a surface of ca. 1 to 4 mm^2 were broken from the grid and put into new petri dishes containing fresh medium and carefully washed with medium 10 times. These glass chips were finally transferred into 24-well plates containing a cell layer of native U-87 MG tumor cells. Dishes were observed on a daily basis for appearance of green cells.

(v) Infection rate. Both high (MOI 50) and low (MOI 1) virus concentrations were used for every virus. To determine the relative number of cells infected for each particular virus, the total number of cells and the number of infected cells were counted in 30 microscope fields based on at least three culture dishes inoculated with each of the nine viruses. Virus infection of the brain tumor-derived cell line U-87 MG was studied through the course of 7 days by analyzing the number of cells expressing the GFP reporter gene as an indicator for infected cells. Since GFP-expressing rMVM would be replication incompetent, we used immunocytochemistry for virus antigen detection as a marker for MVM infection.

(vi) Glioma-fibroblast coculture. In this setting, 10-mm coverslips carrying either glioma cells or human fibroblasts were cut, and one-half from a glioblastoma culture and one-half from a fibroblast culture were placed in the same well of a 24-multiwell dish prior to the addition of the indicated virus suspensions. Each condition was tested in triplicate.

(vii) Virus adaptation to glioblastoma. VSV and SIN were subjected to repeated passaging on a glioblastoma cell culture. First, a monolayer of U-87 MG cells was infected with the original VSV-G–GFP stock at an MOI of 1. Five minutes elapsed for viral attachment, after which the medium was exchanged three times with normal growth medium. Supernatant containing viral progeny was collected at 10 h postinfection (hpi) for the first 10 generations, 8 hpi for the next 10 passages, and 6 hpi for the final passaging rounds. In between each passage, a 1-h incubation on a fibroblast layer was performed to preabsorb virus particles with fibroblast affinity and only the supernatant was passaged. After 30 passages, the virus suspension was double plaque purified, and one clone from a single plaque was expanded, its titer was determined, and it was designated VSV-rp30 (for "30 times repeated passaging"). SIN was passaged on a U-87 MG and M059J coculture with the intention of generating viral progeny with tropism to both glioblastoma lines. The passage time was 24 h.

In vivo experiments. For subcutaneous tumor xenografting, 5×10^5 U-87 MG cells suspended in 100 μl of PBS were injected into each flank of 6- to 8-week-old female CB.17 SCID mice (Jackson Laboratory, Bar Harbor, ME). About 3 weeks after injection, the mean tumor volume (calculated as volume = length × $width^2$ × 0.52) had reached 0.5 ml. For intratumoral injection of the virus, mice were grouped in pairs (four tumors each group) and anesthetized by intramuscular injection of a combination of ketamine and xylazine (100 and 10 mg/kg, respectively). A single bolus of 100 μl containing either 10^{10} transduction units AAV or 10^7 PFU of VSV, VSV-rp30, SIN, or PRV was injected into the center of the tumor mass. The body weight and tumor dimensions were recorded daily. At the indicated time points, mice were sacrificed by an overdose of Nembutal and perfused transcardially with physiological saline, followed by freshly prepared 4% paraformaldehyde solution. Tumor masses were excised and stored in paraformaldehyde. For analyzing viral infection and spread, the tissue block was cut in 20-μm sections by using a microtome. From serial sections, 1 of every 20 sections was mounted in a DAPI (4′,6′-diamidino-2-phenylindole) mounting medium on glass slides for a representative collection of each tumor.

All experiments were performed in accordance with institutional guidelines of the Yale University Animal Care and Use Committee.

Microscopy. An Olympus IX 71 fluorescence microscope was used to analyze fluorescence with 485-nm excitation for GFP detection, 530-nm excitation for red fluorescence, and a triple filter for DAPI with green or red fluorescence. The microscope was connected to a SPOT RT digital camera (Diagnostic Instruments, Sterling Heights, MI) interfaced with an Apple Macintosh computer. All counting steps were done at the computer screen. The contrast and color of the photomicrographs taken were corrected with Adobe Photoshop.

Immunocytochemistry. At the indicated time points, cells were washed with PBS (plus Ca^{2+} and Mg^{2+}) and fixed with 200 μl of 2.5% paraformaldehyde for 15 min at room temperature. Cells were permeabilized with 0.1% Triton X solution for 10 min. After the unspecific binding sites were blocked with 20% normal goat serum (NGS) in PBS for 1 h at room temperature, the cells were incubated with a 1:100 dilution of a polyclonal antibody with reactivity to both MVM NS1 and NS2 for 1 h at 37°C. A 20-min reblock with 20% NGS was followed by an incubation with the FITC-labeled secondary antibody (#111-095-1440; Jackson Immunoresearch Laboratories, West Grove, PA) for 45 min at 37°C. After each antibody incubation, the cells were washed thoroughly with PBS. Immunoreactivity was observed by using a fluorescence microscope. Negative controls were performed by staining mock-infected cells and by excluding the primary antibody. Positive controls included the use of the MVM-permissive cell line 324K and test experiments with a monoclonal primary antibody that revealed a similar pattern of immunoreactivity.

RESULTS

In this study we compared the characteristics of nine viruses infecting human glioblastoma cell lines in vitro and in vivo to analyze their potential as antitumor agents. All viruses tested with the exception of the two MVM strains were recombinant

viruses expressing GFP, allowing clear detection of viral infection and gene expression. In cell culture experiments, we studied the infection rate, antiproliferative effects, tumor cell lysis, and replication capacity. Experiments were repeated on a second human glioblastoma cell line with a different genetic profile to determine whether the results could be generalized to different glioblastoma types. To further examine tumor specificity, we used human fibroblasts as a control and tested the five viruses that showed strong actions against tumor cells with the control cells. In addition, we performed serial passage experiments with the best candidate viruses on glial tumors to potentially enhance their antitumor characteristics. Finally, we tested viruses that worked best in vitro in an in vivo proof-of-principle model with subcutaneous xenografts of human glioblastoma cells in SCID mice.

Assessment of in vitro characteristics of nine viruses. Each set of experiments in the Results section is organized by RNA and DNA viruses, and the order of description is maintained in the different tests, i.e., VSV, SIN, PRV, hCMV, mCMV, MVMi, MVMp, AAV, and SV40.

Infection rate. (i) RNA viruses. VSV infection occurred rapidly, and GFP fluorescence could be observed as early as 4 hpi. The difference between the low (MOI 1) and high (MOI 50) virus concentration was only marginal, and nearly all cells showed GFP expression at 1 day postinfection (dpi). VSV-GFP fluorescence showed a very distinct pattern with prominent membrane fluorescence (Fig. 1A2). By 3 dpi, all remaining cells were green (Fig. 2A). At 5 and 7 dpi, only clusters of cell debris could be detected in the dishes.

GFP expression in SIN-infected glioblastoma cells occurred more slowly than with VSV and in a concentration-dependent manner. The first signs of weak cytosolic GFP expression were observed at about 12 and 16 hpi (MOI 50 and MOI 1, respectively). Green fluorescence gradually increased, and all cells expressed GFP at 5 dpi (MOI 50) or dpi 7 (MOI 1), respectively (Fig. 1B2 and 2B).

(ii) DNA viruses, enveloped. The time course of PRV infection revealed two patterns depending on the initial level of viral load. At MOI 50, GFP expression could be detected as early as 6 hpi, and nearly all cells were infected after 1 dpi (Fig. 1C2, at 7dpi). In contrast, at low virus concentrations GFP expression was considerably lower (Fig. 2C).

The recombinant human CMV strain included in our experiment did not show a strong GFP expression in human U-87 MG cells (Fig. 1D2). GFP-positive cells appeared after 24 hpi and peaked at 5 dpi (7.9% ± 0.7% at MOI 50; Fig. 2D). At an MOI of 1, GFP expression was negligible.

Based on a previous study showing that mCMV infected several cell populations in human hippocampal slices (60), we included mCMV (MC.55) to address its affinity for human glial tumors. The first signs of infection became evident at 24 hpi. Only high infection levels of MOI 50 led to a moderate GFP expression (peak value of 10% at 3 dpi; Fig. 1E2 and 2E).

(iii) DNA viruses, nonenveloped. The two MVM strains tested—MVMi and MVMp–are nonrecombinant virus strains requiring immunostaining for detection (Fig. 1F2 and G2). Immunostaining of MVMi (MOI 50)-infected cells peaked at 3 dpi with ~40%, and immunostaining of MVMp-infected cells peaked at 5 dpi with ~30% (Fig. 2F and G). Infections at lower MOIs caused immunoreactivity in the range of 5 to 10% of cells.

GFP expression in AAV-2-infected U-87 MG cells was limited to the high MOI of 50 and was first detected as early as 10 hpi. GFP labeling peaked on 5 dpi with ~50% of green cells (Fig. 1H2 and 2H).

SV40 did not show a convincing affinity for these human tumor cells. By the end of the 1-week observation, very few cells showed GFP expression (Fig. 1I2 and 2I). In contrast, the recombinant SV40 showed strong GFP expression in control CMT4 cells that provide the large T antigen in *trans*.

Effect on cell proliferation. (i) RNA viruses. VSV at both MOIs significantly reduced the number of tumor cells within 24 hpi. Cell numbers dropped to only a few cells within the next 2 days. By 5 and 7 dpi, we could not detect any viable cells in any VSV-infected dish (Fig. 2A). In contrast, cell numbers in mock-infected dishes doubled about every second day generating a smooth exponential growth curve.

By 1 dpi, SIN showed substantial growth suppression in dishes with the higher viral load (MOI 50). Cell numbers remained basically at the initial levels, dropping continuously over the course of the next 4 days, and reached zero by the end of the 1-week observation period. At the lower virus concentration, the suppressing effect of SIN on tumor cell proliferation was delayed and came into effect after 3 dpi.

(ii) DNA viruses, enveloped. Proliferation of U-87 MG cell cultures was significantly halted by PRV at MOI 50 at 1 and 3 dpi (Fig. 2C). After 1 week, cell numbers were reduced to ~30%. In contrast, low PRV concentration of MOI 1 could only slightly suppress the cell growth. At 7 dpi, the cells had grown to full confluency, although they were not as dense as the overgrown control culture.

Infection of U-87 MG cells by either human or mouse CMV did not result in any significant effect on the proliferation rate, as can be seen by the matching growth curves in Fig. 2D and E.

(iii) DNA viruses, nonenveloped. At the higher concentration, MVMi infection resulted in a substantial block of culture growth, with cell numbers falling to ~80% (Fig. 2F) of the initial levels on 5 dpi. Interestingly, tumor cells showed a tendency toward recovery at 7 dpi, with a slowly increasing growth rate. On the other hand, MVMp infection at MOI 50 caused only a moderate slowing down of tumor cell proliferation (Fig. 2G). Based on the rising cell number in both MVM dishes by the end of the 1-week surveillance, we introduced an additional observation point at 13 dpi to analyze whether the growth suppressing effects of MVM were sustainable. In fact, the cell growth rate in MVMi-infected dishes reached 477.0% ± 47.5% at 13 dpi, revealing that a single application was not enough to block cell growth over an extended period. MVMp-infected cultures were overgrown by day 13, and cell numbers increased to 20-fold of the initial cell count (2,088% ± 269.0%; $n = 30$ fields). With an MOI of 1, MVM strains did not differ significantly and showed only a mild suppression of the growth curve.

The two remaining recombinant viruses, AAV-2 and SV40, did not show any effect on the proliferation of U-87 MG cells (Fig. 2H and I). These cell proliferation and cytopathic effect (CPE) studies were repeated with wild-type, replication-competent SV40 virus with essentially identical results.

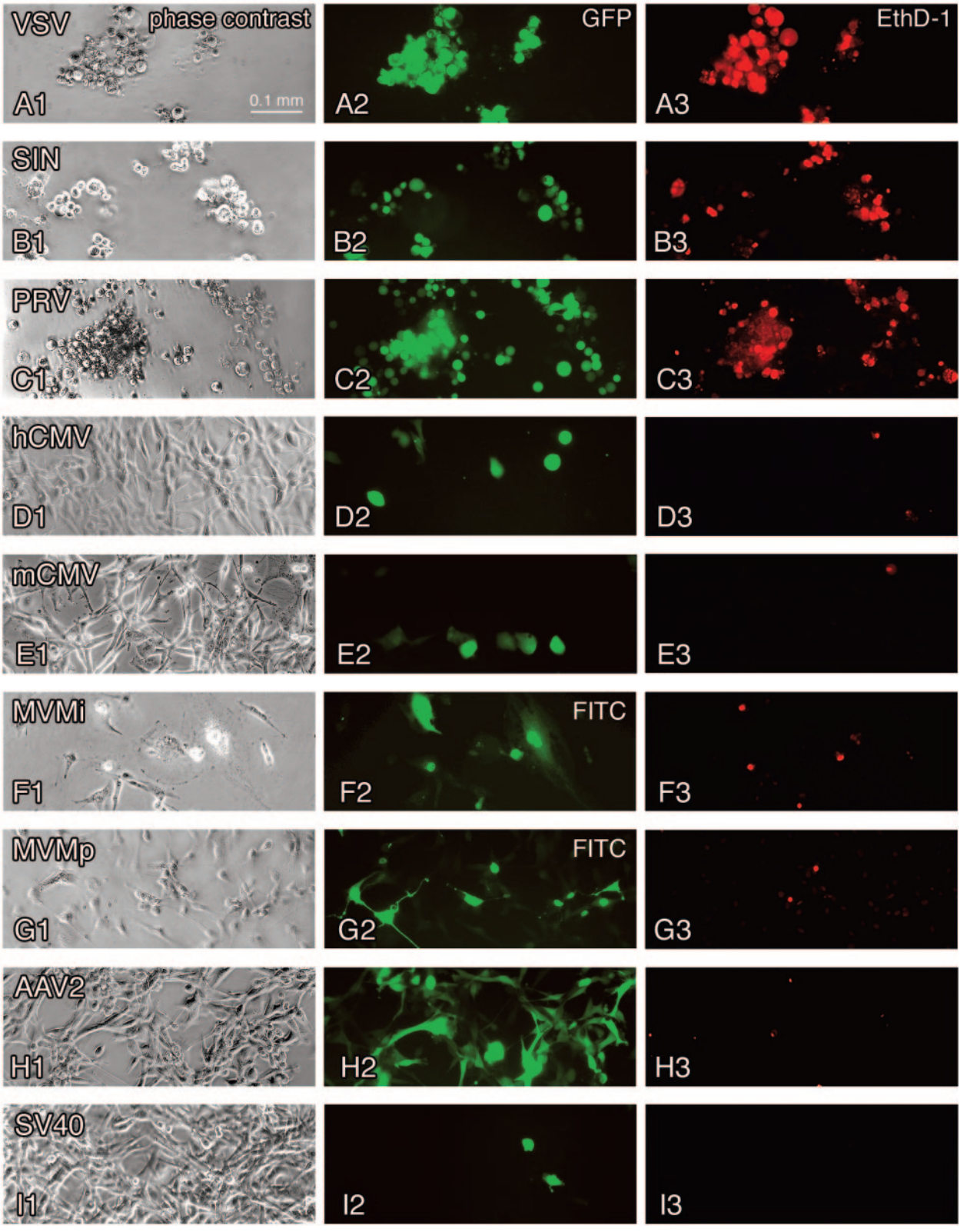

FIG. 1. Virus infection, transgene expression, and cytolytic action in human glioblastoma cells. Representative effects of seven recombinant GFP-expressing viruses and two strains of MVM are depicted in this panel showing phase-contrast (first column), green GFP fluorescence (second column), and EthD-1 cell death staining (third column) in corresponding visual fields after U-87 MG inoculation. All cultures were infected at an initial MOI of 50. (A) Infection with VSV after 24 h. (B) SIN infection at 3 dpi. (C) PRV infection at 7 dpi. (D) Infection with human CMV at 5 dpi. A small number of cells accumulate high levels of GFP and show CPEs. (E) Infection with mouse CMV at 3 dpi. Green cells appeared mostly with normal morphology. The cellular GFP expression was weak. (F) MVMi infection at 3 dpi. Immunocytochemistry revealed predominantly nuclear staining of viral proteins NS1/NS2. (G) MVMp infection at 5 dpi. (H) Infection with AAV2 at 5 dpi. (I) Infection with SV40 at 7 dpi.

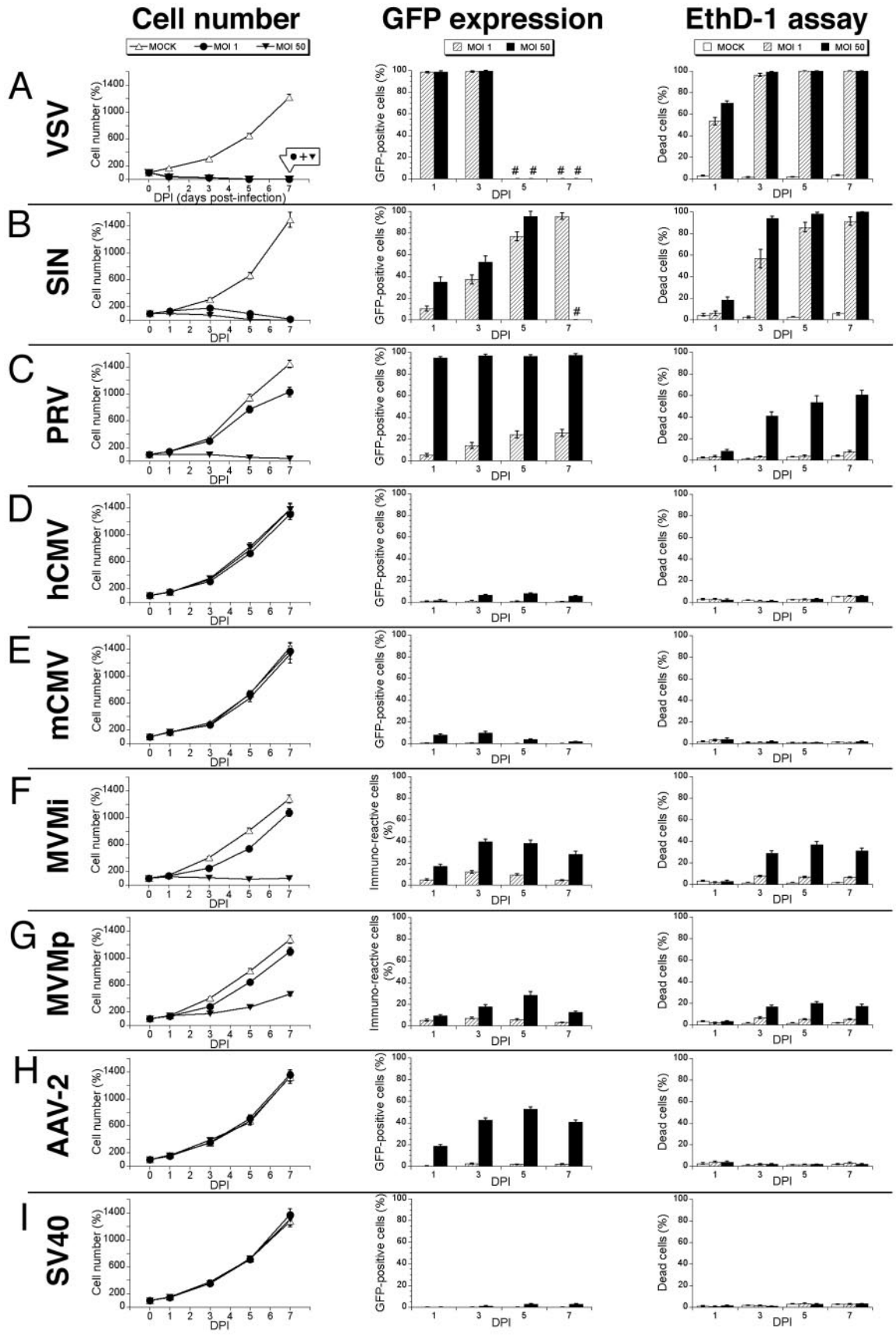
Cell number
GFP expression
EthD-1 assay
MOCK
MOI 1
MOI 50
A
VSV
B
SIN
C
PRV
D
hCMV
E
mCMV
F
MVMi
G
MVMp
H
AAV-2
I
SV40
Cell number (%)
GFP-positive cells (%)
Immuno-reactive cells (%)
Dead cells (%)
DPI
DPI (days post-infection)

Cytotoxic effects. Virus inhibition of cell growth could occur through several different mechanisms. To test whether the viruses described above that slowed tumor growth did so by cytolytic actions, we studied cell death by using an ethidium homodimer cell death assay at 1, 3, 5, and 7 dpi. In addition, cell cultures were screened for the occurrence of CPEs.

(i) RNA viruses. VSV infection caused substantial CPEs in the form of rounding up, detachment, and membrane blebbing, which started as early as 6 hpi. At 1 dpi, more than half of the cells in both cultures stained red in the EthD-1 assay (Fig. 1A3), revealing dead or dying cells. By 3 dpi, nearly all of the cells exhibited red nuclear fluorescence (Fig. 2A).

Cells infected with SIN presented marked CPEs in the form of rounding up and monolayer disruption. At 24 hpi, EthD-1 staining revealed moderate rates of cell death at MOI 50 but no effect at MOI 1. At the following time points, nearly all cells initially infected with MOI 50 showed red nuclear fluorescence (Fig. 1B3 and 2B). At an MOI of 1, cell death rates rose to >90% by 7 dpi.

(ii) DNA viruses, enveloped. PRV-infected cells presented CPEs (rounding up and detachment) ca. 24 h after cells started to express GFP. In the course of 1 week, EthD-1 positivity rates rose steadily up to ca. 60%, with concomitantly dropping cell numbers at high initial infectious titers (MOI 50) (Fig. 1C3). In contrast, low virus titers did not result in substantial cell death (Fig. 2C).

hCMV infection did not cause an increase in EthD-1 monitored cell death (Fig. 1D3 and 2D). The GFP-positive cells showed occasional signs of CPE (rounding up); syncytium formation was observed in just 1 out of 30 fields. Infection with mouse CMV also did not result in any detectable increase in cell death by means of EthD-1 labeling (Fig. 1E3 and 2E).

(iii) DNA viruses, nonenveloped. CPEs associated with MVM infection included rounding up and detachment. EthD-1 labeling peaked at 5 dpi with ~40% in MVMi (MOI 50)-infected cultures and with ~20% in MVMp (MOI 50)-infected cultures (Fig. 1F3 and G3). At a lower initial viral load (MOI 1), both virus strains caused cell death in ca. 5 to 8% between 3 and 7 dpi (Fig. 2F plus G). Thirteen days after treatment the recovery of cell proliferation in both cultures was reflected in a significant drop in cell death rates (17.8% ± 0.8% in MVMi cultures and 7.7% ± 0.3% in MVMp cultures), indicating that a single application of MVM did not sustain its tumor-suppressive action.

AAV2 and SV40 infection did not cause any morphological change or cell death during the 1-week observation period (Fig. 1H3, 2H, 1I3, and 2I). For control purposes, U-87 MG cells were also infected with wild-type SV40. Wild-type SV40 showed no increased cytotoxicity.

Viral replication and spread. To address the question of whether a virus could replicate in infected glioma cells and progeny spread to cells not initially infected, we introduced a straightforward replication assay on the basis of transferring infected cells growing on a glass chip to a noninfected culture. Test determinants were the appearance of infected cells in the monolayer and a potential effect on the intactness of the monolayer (Fig. 3F).

(i) RNA viruses. The first signs of VSV-induced GFP expression among cells in the initially uninfected host chamber appeared about 12 h after transfer of the glass chip. At 24 h, >50% of the host cells expressed GFP. By day 3, VSV had spread throughout the whole culture in all dishes, as detected by strong GFP expression in all host cells, inflicting strong CPEs in all cells and subsequently causing cell death (Fig. 3A). VSV caused a complete destruction of cells in the host chamber by day 5.

Upon studying SIN replication, we found that GFP-expressing cells appeared at 5 dpi throughout the monolayer (two dishes with ~80% green cells and one dish with ~50% green cells; Fig. 3B). Infection was accompanied by marked CPEs in the form of rounding up and detachment. By dpi 7, the monolayer was disrupted and the number of cells was noticeably reduced, demonstrating a successful replication of SIN and an amplification of the tumor-suppressive effect.

(ii) DNA viruses, enveloped. At 1 dpi, PRV-infected cells on the glass chip showed GFP fluorescence. One day later, the first green cells appeared in proximity to the glass chip. In the course of the 1-week observation period, GFP-expressing cells spread through the monolayer in a sequential fashion, suggesting a cell-to-cell transmission rather than a free release into the medium (Fig. 3C). The effect on the integrity of the monolayer was moderate: although strong CPEs resulting in cell death were inflicted in areas of PRV spread, the culture was maintained and grew to full confluency, disrupted only by small green patches. Thus, U-87 MG cells are permissive for PRV replication, although with a low virus replication index.

After infection with hCMV of cells on the glass chip, the initially treated cells on the glass chip showed GFP fluorescence beginning at 1 dpi, but no GFP expression was observed in the host monolayer throughout the rest of the observation period (Fig. 3D). We conclude that human glioma U-87 MG cells are nonpermissive for hCMV. As expected, human glioma cells U-87 MG were also nonpermissive for the replication of mouse CMV. Green cells became visible on the glass chip as early as 1 dpi, but the monolayer remained clear of any GFP fluorescence throughout the observation period of 9 days.

(iii) DNA viruses, nonenveloped. Three days after a glass chip carrying MVMi-infected U-87 MG cells was placed into a

FIG. 2. Growth curves, fluorescence detection, and cell death analysis. U-87 MG cells were infected at an MOI of 1 or 50 or not infected (MOCK). The data are presented as means ± the standard errors of the mean. (A) VSV rapidly infected and killed glioblastoma cells regardless of the initial viral concentration, leading to nearly identical growth curve suppression by both MOIs. #, Lack of any viable cells. (B) Upon SIN infection tumor cells stop dividing and ultimately died. Some dead cells might have lost their cytosolic GFP through diffusion explaining the higher EthD-1 values. (C) PRV exerts a tumor-suppressive effect at a higher MOI. (D and E) Human (D) or mouse (E) CMV infection did not affect tumor cell growth. (F) MVMi infection stops tumor cell growth at a high MOI. (G) MVMp infection at MOI 50 moderately slows down tumor progression. (H) AAV2 showed considerable infectivity at MOI 50 without disturbing cell viability. (I) Very low infection rates of SV40 at MOI 50.

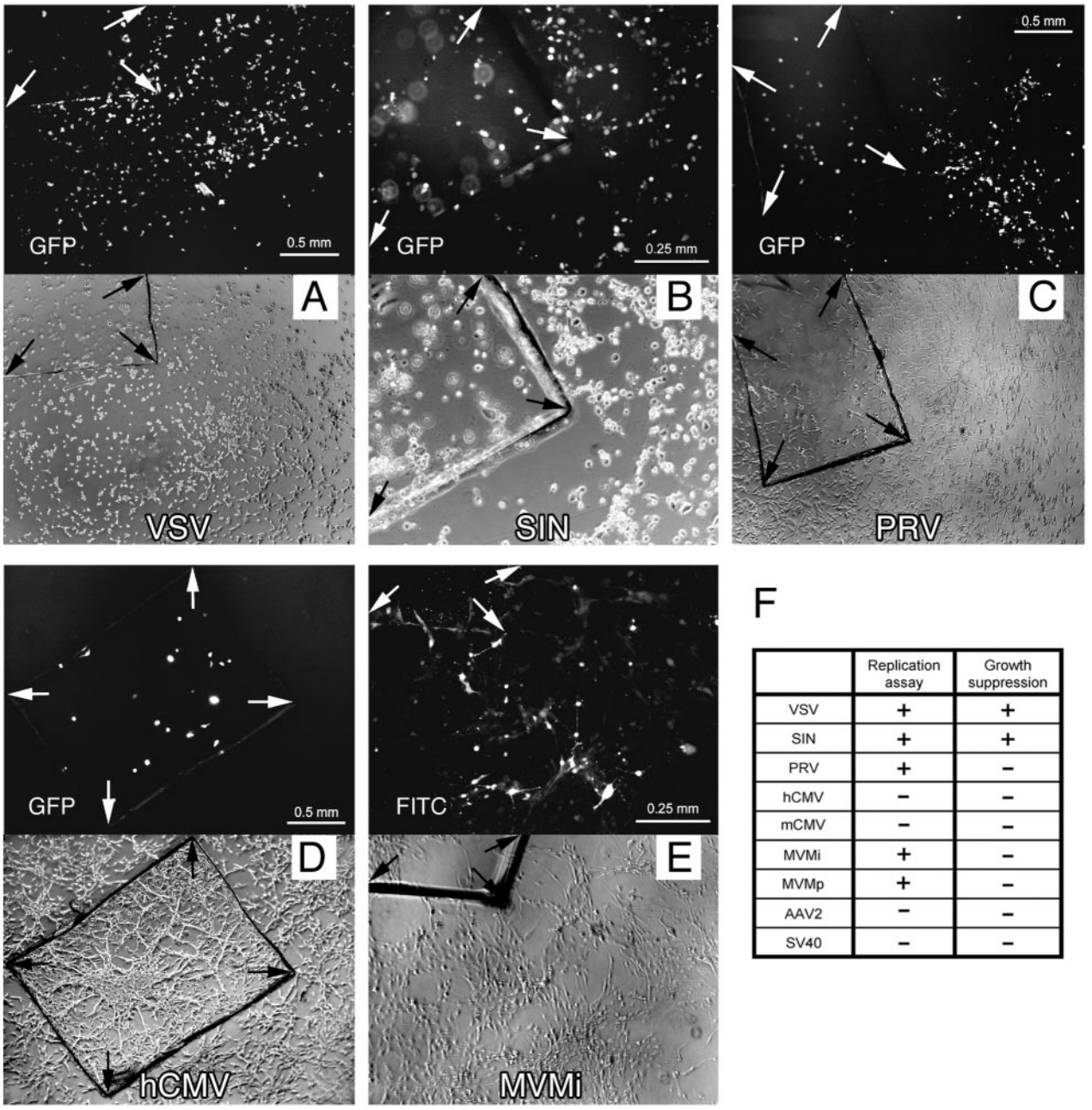

F

	Replication assay	Growth suppression
VSV	+	+
SIN	+	+
PRV	+	−
hCMV	−	−
mCMV	−	−
MVMi	+	−
MVMp	+	−
AAV2	−	−
SV40	−	−

FIG. 3. Virus replication and spread. Small glass chips carrying infected U-87 MG cells were washed and transferred onto a native U-87 MG cell layer. Each set of photomicrographs depicts corresponding fields of fluorescence and phase contrast. (A) Widespread GFP expression after VSV infection in the culture dish at 1 dpi. (B) Replication of SIN was observed with a 3-day latency, inflicting extensive cell death throughout the culture. Due to the different plane, cells located on the glass chip are out of focus. (C) PRV spread to close areas in a fanning-out fashion, indicating a potential cell-to-cell distribution. The integrity of the monolayer was not affected. (D) Human CMV did not replicate and spread. (E) MVMi immunopositive cells were detected at 3 dpi in the area fringing the glass chip. At later time points, groups of cells remote from the glass chip stained positive for MVM infection. (F) Table summarizing virus replication and the effect on the growth of U-87 MG monolayer.

dish with an uninfected U-87 MG monolayer, immunostaining revealed marked cells fringing the glass chip (Fig. 3E). The pattern of immunopositivity expanded throughout the following days, and stained cells could be observed in places remote to the glass chip. However, the overall number of infected cells (ca. 200 to 300) was small in comparison to a confluent monolayer comprised of ca. 200,000 cells, consequently making the adverse effect on the integrity of the cell culture negligible. Replication of MVMp in U-87 MG cells occurred in a similar fashion, although fewer cells were infected by MVMp than by MVMi.

AAV-2 was used as a nonreplicating control, testing whether any unincorporated virus could be transferred with the glass chip. In three dishes with two glass chips each, we did not

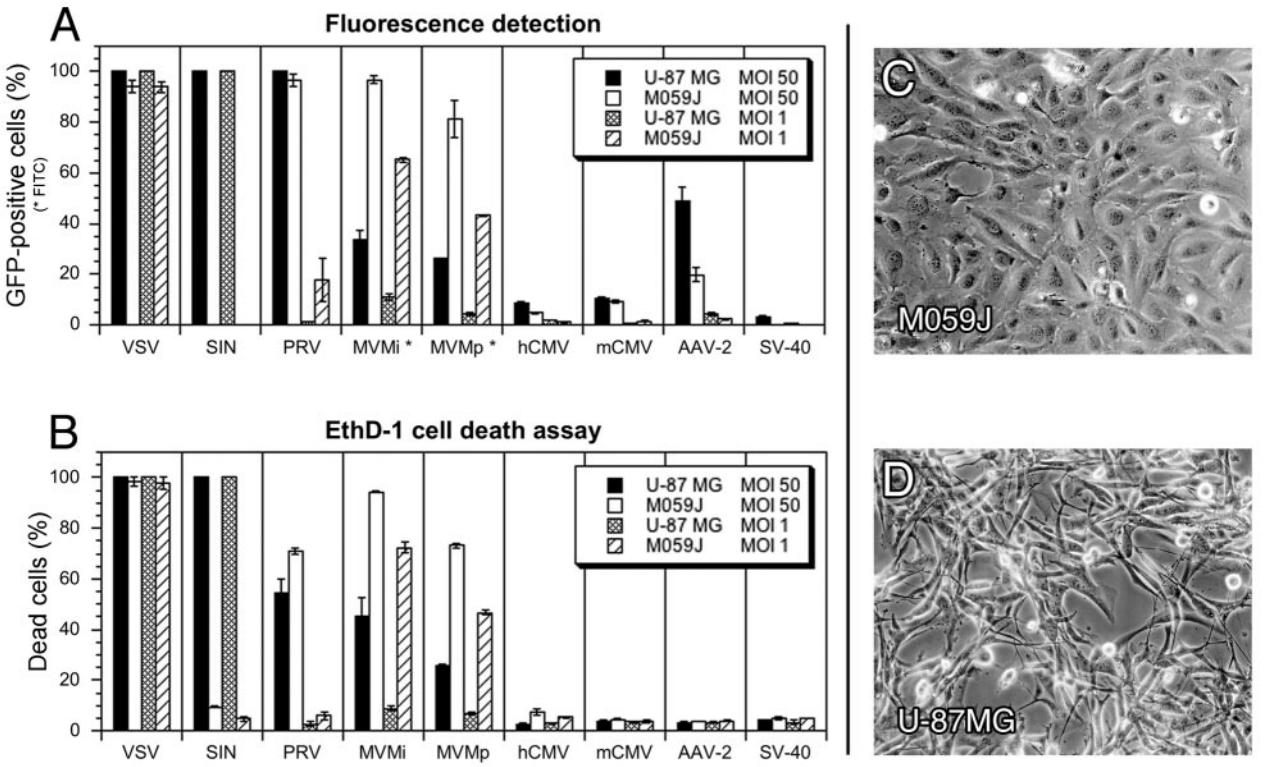

FIG. 4. Generalization in different human glioblastoma lineages of virus infectivity and cytolysis. Two different glioblastoma cell lines were compared for viral infection and associated cytotoxicity. Analysis was carried out at 3 dpi for VSV and at 5 dpi for the other viruses. The data represent means ± the standard errors of the mean. (A) Considerable differences in tropism were observed with SIN, MVMi, and MVMp and to a smaller extent with PRV and AAV. (B) Different cytolytic potential of SIN and both MVM strains showed strong correlation to infectivity. (C) Photomicrograph depicts the typical cell morphology of M059J cells in 5-day-old cultures. (D) Typical image of U-87 MG cells after 5 days in culture.

observe any GFP fluorescence in the monolayer throughout the 9-day observation period, although most of the cells on the transfer chip were bright green. The AAV data support the view that this approach functions as a viable indicator for viral replication in vitro.

SV40-inoculated GFP-positive cells appeared on the glass chip at 3 dpi. In contrast, the monolayer culture remained clear of any signs of GFP expression through the 9-day observation period, as expected for this recombinant form of SV40 that is incapable of propagation in the absence of viral T antigen.

Virus generalization to glioblastoma cell line with different derivation. Experiments addressing the infection rate, cell death, and viral replication were repeated with a different glioblastoma cell line M059J (Fig. 4C), and the profiles of antitumor activities were compared. A different set of genetic lesions underlies the transformation of M059J compared to U-87 MG as detailed in the Discussion. Analysis was performed at 5 dpi for most viruses and at 3 dpi for VSV due to its rapid action. Graphs summarizing experiments for green fluorescence detection and EthD-1 cell death assay are presented in Fig. 4.

(i) RNA viruses. VSV infection of M059J cells led to a rapid and widespread expression of GFP, following a time course similar to U-87 MG cells. Similar to the U-87 MG cells, M059J cells were fully permissive for viral replication. Although a marginal difference, the effect of VSV on M059J cells was slightly delayed compared to that on U-87 MG cells.

Surprisingly, SIN did not infect M059J cells. There were neither signs of GFP expression nor any adverse effects on cell growth or vitality. For control purposes, we repeated the experiments with U-87 MG and confirmed the cytotoxic results described above. Hence, we conclude that M059J is nonpermissive and that U-87 MG is fully permissive for SIN infection, indicating an involvement of distinguishing factors for virus entry or viral gene expression in two glioblastoma cell lines.

(ii) DNA viruses, enveloped. PRV infection of M059J cells with initial levels of 50 MOI resulted in GFP expression in almost the entire culture, mirroring the strong effect of PRV on U-87 MG cells. However, at a lower dose of 1 MOI, M059J cells were much more susceptible to PRV infection than were U-87 MG cells (18% versus 2%). This trend was reproduced in the EthD-1 cell death assay with a higher labeling index in M059J cultures than in U-87 MG cultures for both viral concentrations, as well as in the replication assay with a higher replication index in M059J cells.

Infection of M059J cells by either human or mouse CMV resulted in low numbers of GFP-expressing cells, with results comparable to those obtained for infected U-87 MG cells. Cell death rates did not differ from mock-infected cultures. As in

U-87 MG cells, we did not observe any evidence of viral replication.

(iii) DNA viruses, nonenveloped. MVM was significantly more effective at infecting M059J cultures than those of U-87 MG. At the high viral concentration (50 MOI), immunostaining at 5 dpi revealed an infection rate in M059J cultures approximately double the rates found in U-87 MG cultures, leading to ~95% labeled cells with the MVMi strain and ~80% labeled cells with the MVMp strain. Parallel values were found in the EthD-1 assay. The difference between the two cell lines became even more evident when a lower viral dose was applied (1 MOI). Values for immunostaining and EthD-1 labeling of infected M059J cells were approximately four times greater than in U-87 MG cultures. In addition, M059J cells showed higher rates of replication for both MVM strains compared to U-87 MG cells. Confirming experiments described in the previous paragraphs, MVMi exhibited a stronger infectivity and cytotoxic profile than MVMp.

AAV-2 exhibited a lower affinity for M059J cells than for U-87 MG cells. At 5 dpi, infection (MOI 50) resulted in ca. 20% GFP positivity in M059J cells compared to ca. 50% in U-87 MG cells. EthD-1 labeling did not differ from mock-infected cultures.

M059J cultures exposed to SV40 did not express GFP, further substantiating the low efficiency of infection of this recombinant SV40 in human glial tumor cell lines.

Effect on nonglioblastoma control cells. Based on the experiments above, five viruses from the initial set emerged as potential antiglioblastoma agents: VSV, SIN, PRV, and the two MVM strains. To test whether the viruses showed any selective affinity for glioblastoma cells, normal human adult fibroblasts were cocultured with U-87 MG cells and exposed to either MOI 1 or MOI 10.

After VSV infection, the first signs of GFP expression were detected at 6 hpi in tumor cells but only after 18 hpi in human fibroblasts. At 1 dpi, all tumor cells showed green fluorescence (Fig. 5A) compared to 50% GFP positivity among the fibroblast culture (Fig. 5B). At 3 dpi, ca. 80% of fibroblasts expressed GFP. The initial MOI did not seem to influence the course of GFP expression, which is most likely explainable by the large amount of virus progeny released rapidly by infected tumor cells.

Human fibroblasts did not show any signs of infection with SIN. During the 1-week observation period fibroblasts remained clear of any CPEs and GFP expression at both infectivity levels MOI 1 and MOI 10 (Fig. 5C). Simultaneously, U-87 MG cells were effectively infected by SIN, reproducing the tumor-suppressive outcome described in the previous paragraphs. We conclude that these normal human fibroblasts are nonpermissive for SIN infection.

PRV infection of cocultured U-87 MG cells and normal human fibroblasts led to GFP expression and consecutive CPEs in both cell types. At initial virus levels of MOI 10, 50% of the cells in both groups expressed GFP after 24 h and ca. 90% expressed GFP at 3 dpi. Of note, fibroblasts appeared to be more susceptible to viral infection than glioblastoma cells at a low MOI (human fibroblasts, ~50% at 3 dpi [Fig. 5D]; U-87 MG, ~10% at 3 dpi). Infected tumor cells rapidly exhibited pronounced CPEs, whereas a 2-day delay was observed for morphological changes of infected fibroblasts.

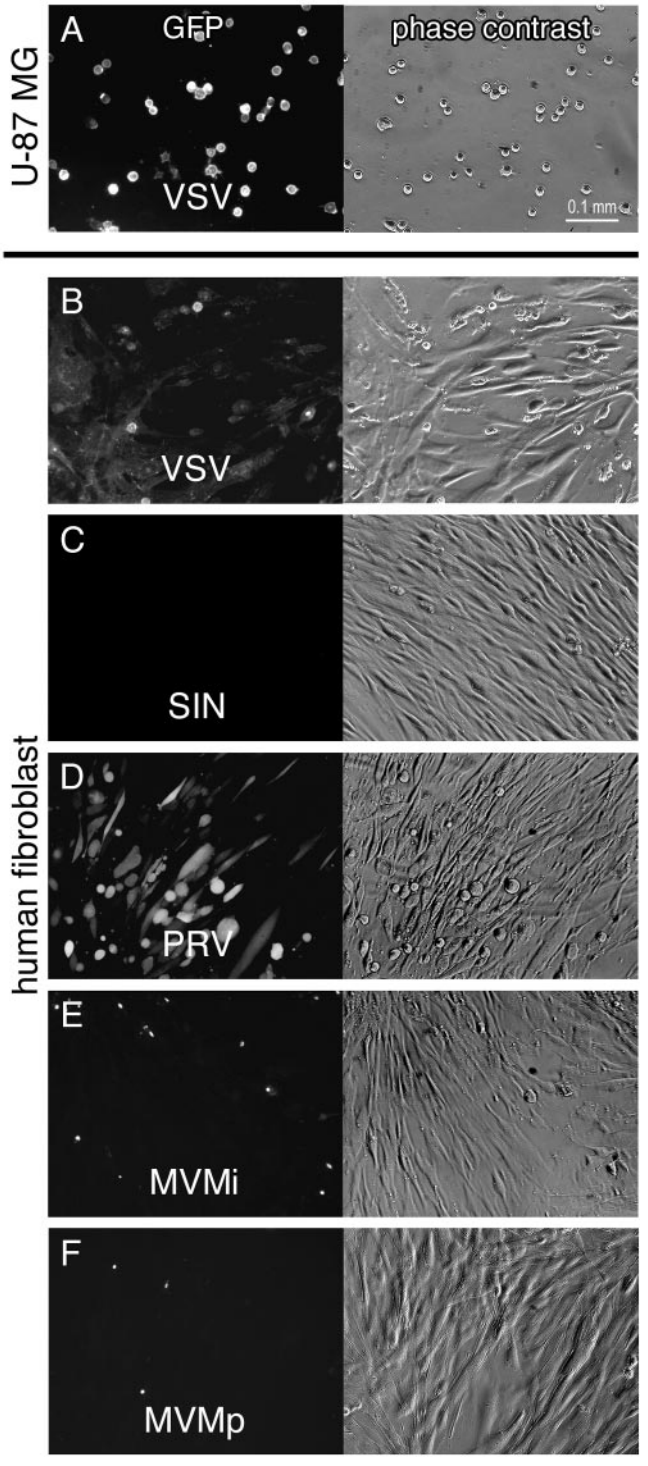

FIG. 5. Infection of cocultured human glioblastoma and control fibroblasts. Images show phase-contrast and GFP expression or fluorescein isothiocyanate (FITC) staining of human fibroblasts cocultured withU-87 MG cells in the same dish. The virus concentration was MOI 1. (A) At 24 h after VSV infection, all tumor cells showed GFP expression and CPEs. (B) In the same dish, some fibroblasts showed GFP expression. (C) SIN infection at 3 dpi, with no signs of infection among the fibroblast cells. (D) Preferential infection of human fibroblasts by PRV at 3 dpi. (E and F) Few signs of infection with MVMi and MVMp among human fibroblasts. Images were taken after immunocytochemistry at 3 dpi.

HCMV showed little infection of human glioblastoma cells. To test that the virus maintained replication potential in other cells, we tested the recombinant on human fibroblasts. HCMV rapidly infected cultured fibroblasts as indicated by GFP expression, caused CPEs and cell death (data not shown). Based on the same test principle as our glass chip replication assay, hCMV effectively produced progenitors that ultimately destroyed the fibroblast monolayer (data not shown).

Immunocytochemistry for MVM antigen detection was performed 3 and 7 dpi. At both time points, labeling for viral infected cells was very sparse among the fibroblast monolayer, resulting in ca. 1 to 2% positive cells after MVMp exposure (MOI 1) and <5% with MVMi (MOI 1)-exposed cultures (Fig. 5E and F). Interestingly, a higher MOI of 10 did not result in increased labeling indices of fibroblast cultures. In addition, no morphological changes were observed in fibroblasts. Infection rates of MVM in U-87 MG cultures were comparable to the numbers presented in Fig. 2F and G and in the results presented above.

Adaptation of viruses through repeated passaging. RNA viruses are prone to spontaneous genetic variation. The mutation rate of VSV is ca. 10^{-4} per nucleotide replicated, giving ~1 change per genome (15). This provides the basis for a viral capacity to adapt to changing cellular environments. The VSV strain used in the present study rapidly killed tumor cells; however, its cytotoxic potential was not limited to tumor cells, as was shown by delayed infection of normal human fibroblasts. Through repeated passaging under certain enforcing conditions, we tested the hypothesis that VSV could be adapted to human glioblastoma cells with reduced affinity for control human fibroblasts.

Since the recombinant VSV strain (VSV-G/GFP) was originally grown on BHK-21 cells, we adapted it to U-87 MG cells by repeated serial passaging (30 times) and enhancing selection through several mechanisms: (i) short time for viral attachment to glioma cells, (ii) collection of early viral progeny, and (iii) preabsorption of viral particles with high fibroblast affinity. The results comparing the original VSV-G/GFP with the glioma-adapted VSV-rp30 are presented in Fig. 6 and 7. To ensure equal virus titers, a plaque assay was performed prior to each experiment with dilutions of the viral working solutions (Fig. 7A). To test whether a potential tumor cell adaptation would result in an enhanced infectivity not only to the passage cell line but also to a variety of different glioblastoma cell lines, we compared the original VSV-G/GFP and VSV-rp30 on five distinctive glioblastoma cell lines (U-87, M059J, U-118, A-172, and U-373). Early during the infection, VSV-rp30 consistently infected all tested glioblastoma cell lines more rapidly than VSV-G/GFP, as shown by the stronger appearance of GFP and CPEs (Fig. 6A). Figure 6B summarizes the comparison of infection with VSV and VSV-rp30 during the first 12 h of infection with an MOI of 10. Ten microscopic fields from two dishes for each condition were analyzed.

Human fibroblasts were used as control cells to study the oncotropism of VSV. VSV-rp30 showed signs of attenuation for infection of human fibroblasts. Throughout a 1-week observation period, human fibroblast monolayers remained intact at low VSV-rp30 concentrations (MOI 0.1 and MOI 1) compared to an overall cell death caused by infection with VSV-G/GFP (Fig. 7B). At higher viral concentrations (MOI 10), however, VSV-rp30 caused cell death to normal human fibroblasts, although at a slower rate than normal VSV-G/GFP (data not shown). To verify this trend of increased specificity, a coculture was used in which small glass chips carrying U-87 MG cells were placed onto a confluent fibroblast monolayer prior to adding a virus suspension containing 10^5 PFU. Figure 7C presents typical images taken at an early and late time point. At dpi 1, both VSV strains produced GFP expression in all U-87 MG cells (located on the glass chip). In contrast, the fibroblast monolayer remained clear of any GFP expression in VSV-rp30 dishes but showed substantial GFP expression in VSV-G/GFP dishes. This pattern was confirmed by observations at dpi 7. VSV-G/GFP caused an overall cell death producing green cell debris of glioblastoma cells and fibroblasts covering the base of the dish, whereas VSV-rp30 selectively killed tumor cells on the glass chip while not affecting the intactness of the fibroblast layer. Together, this approach resulted in a strain that showed an enhanced cytotoxicity and selective affinity for glioblastoma cell compared to control cells.

We used a similar approach for growing successive generations of SIN on glioblastoma cells (including mixed M059J-U87 MG cultures), but the resultant viral progeny behaved similarly to the original stock and therefore is not discussed further here.

Effect of viruses on solid tumor grafts in vivo. In a proof-of-principle study to address the correlation of in vitro results with intratumoral spread, the four viruses with the strongest antitumoral profile in vitro, namely, VSV, its passage-adapted variant VSV-rp30, SIN, and PRV, were injected (10^6 PFU) into subcutaneous solid glioma tumors in two mice each. In addition, GFP-expressing AAV (10^9 transduction units per injection) was included as a replication-incompetent control virus.

Four mice were injected with VSV-G/GFP or VSV-rp30. Analysis of the freshly excised tissue blocks under a fluorescence dissecting microscope revealed widespread GFP expression in the tumor mass but not in the surrounding normal subcutaneous tissue. In two mice bearing pairs of tumors, only one of the tumors was injected with virus. Of interest, both the inoculated and the noninoculated tumors on the opposite side of the body showed a complete green fluorescence at 10 dpi (Fig. 8A), indicating virus spread to tumor tissue in remote places. Microscopic analysis of tumor sections confirmed the tumor specificity. VSV rapidly penetrated the tumor bulk, as was seen 3 and 6 days after VSV or VSV-rp30 inoculation in two tumor samples each. At 10 days after tumor inoculation, VSV-G/GFP (Fig. 8B, corresponding to Fig. 8A) and VSV-rp30 (Fig. 8C) had reached the outermost tumor cell layers but did not spread into the surrounding normal tissue, as can be seen by the clear border demarcation. In addition, clear cytopathic changes in the form of loss of cellular processes and cellular rounding were present.

After SIN inoculation (10 dpi), GFP fluorescence showed a widely distributed pattern with multiple small plaques throughout the tumor tissue. In addition, a distinct subcapsular band of green fluorescence was present in both tumors (Fig. 8D). At high magnification, half of the infected cells exhibited cytolytic morphological changes, including cellular rounding and cellular disintegration with formation of small green granules.

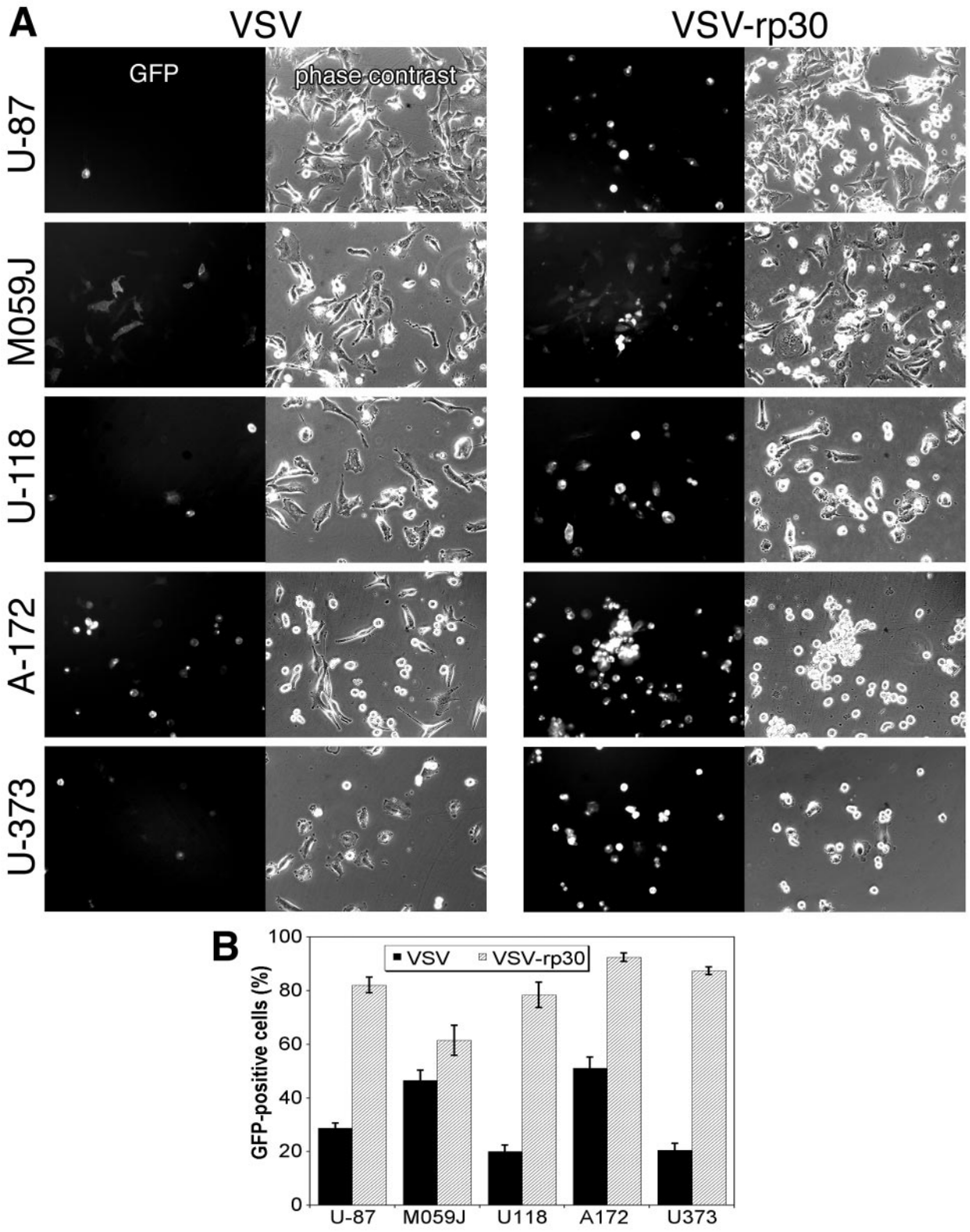

FIG. 6. Glioblastoma-adapted VSV-rp30: enhanced targeting of diverse glioma phenotypes. The glioblastoma-adapted strain VSV-rp30 was compared to the original VSV-G/GFP. (A) VSV-rp30 presents a strong tropism for numerous tested glioblastoma cell lines. Representative photomicrographs are shown here for U-87 MG, M059J, U-118 MG, A-172, and U-373 MG cells. The MOI for VSV and VSV-rp30 was 10. (B) Bar graph comparing the infection rates of VSV and VSV-rp30 on U-373, A-172, U-118, M059J, and U-87 at 10 MOI. Values represent mean of 10 microscopic fields. In each cell line, pairs of micrographs showing VSV or VSV-rp30 and analysis of cell infection were made at the same time postinoculation (<12 h).

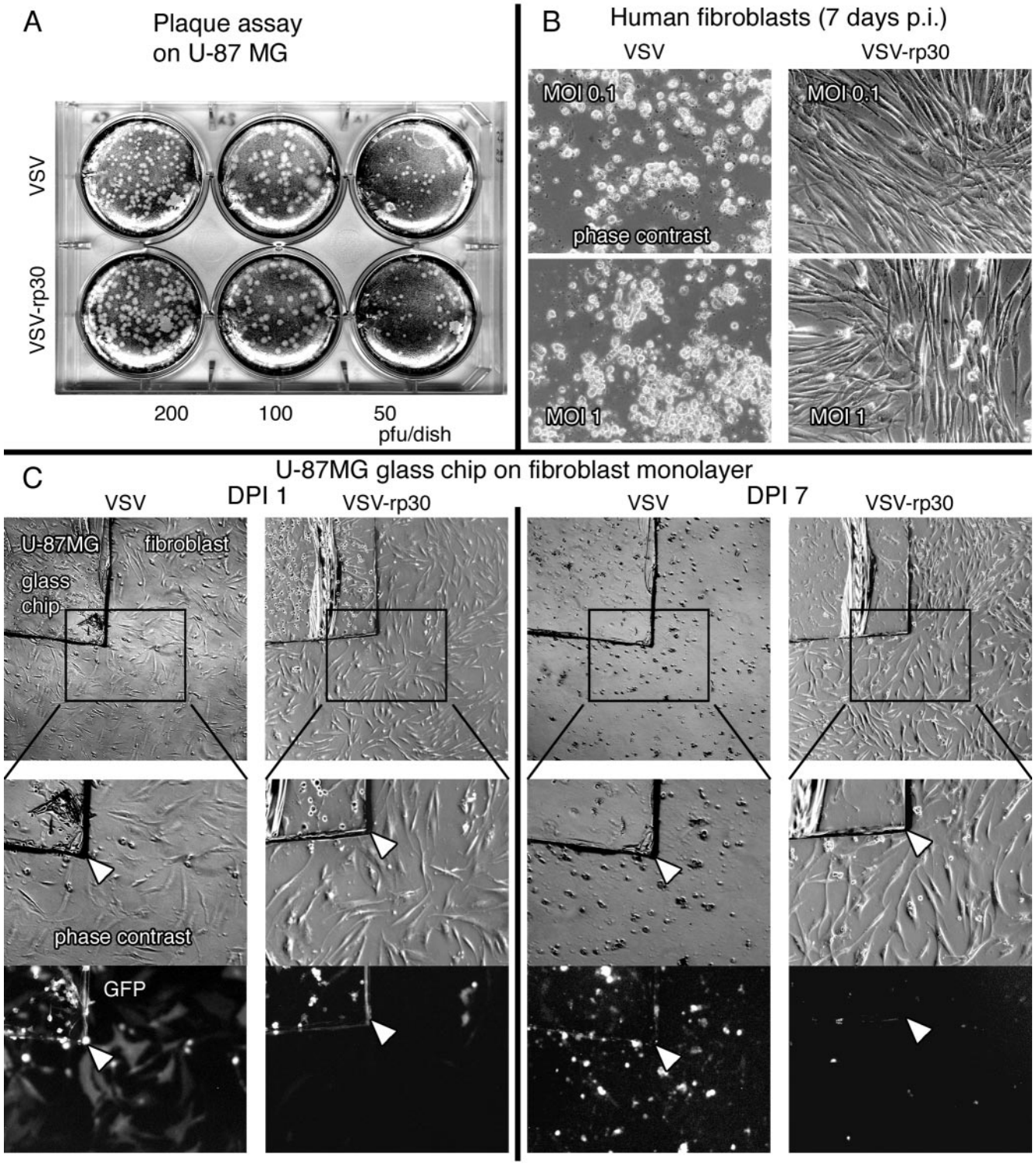

FIG. 7. Glioblastoma-adapted VSV-rp30: attenuation of control cell infection. (A) Virus suspensions were tested with plaque assays prior to each experiment to ensure equal viral load for this comparative study. (B) VSV-rp30 was considerably attenuated for infection and cytotoxicity of normal human fibroblasts compared to the original VSV. (C) Coculture infection. Tumor cells were grown on a glass chip and transferred onto a fibroblast layer prior to adding either VSV-G/GFP or VSV-rp30 at an MOI of 1. The photomicrographs illustrate patterns of GFP expression and presence of cytopathic effects at 24 hpi (two left columns) and the long-term outcome at 7 dpi (two right columns).

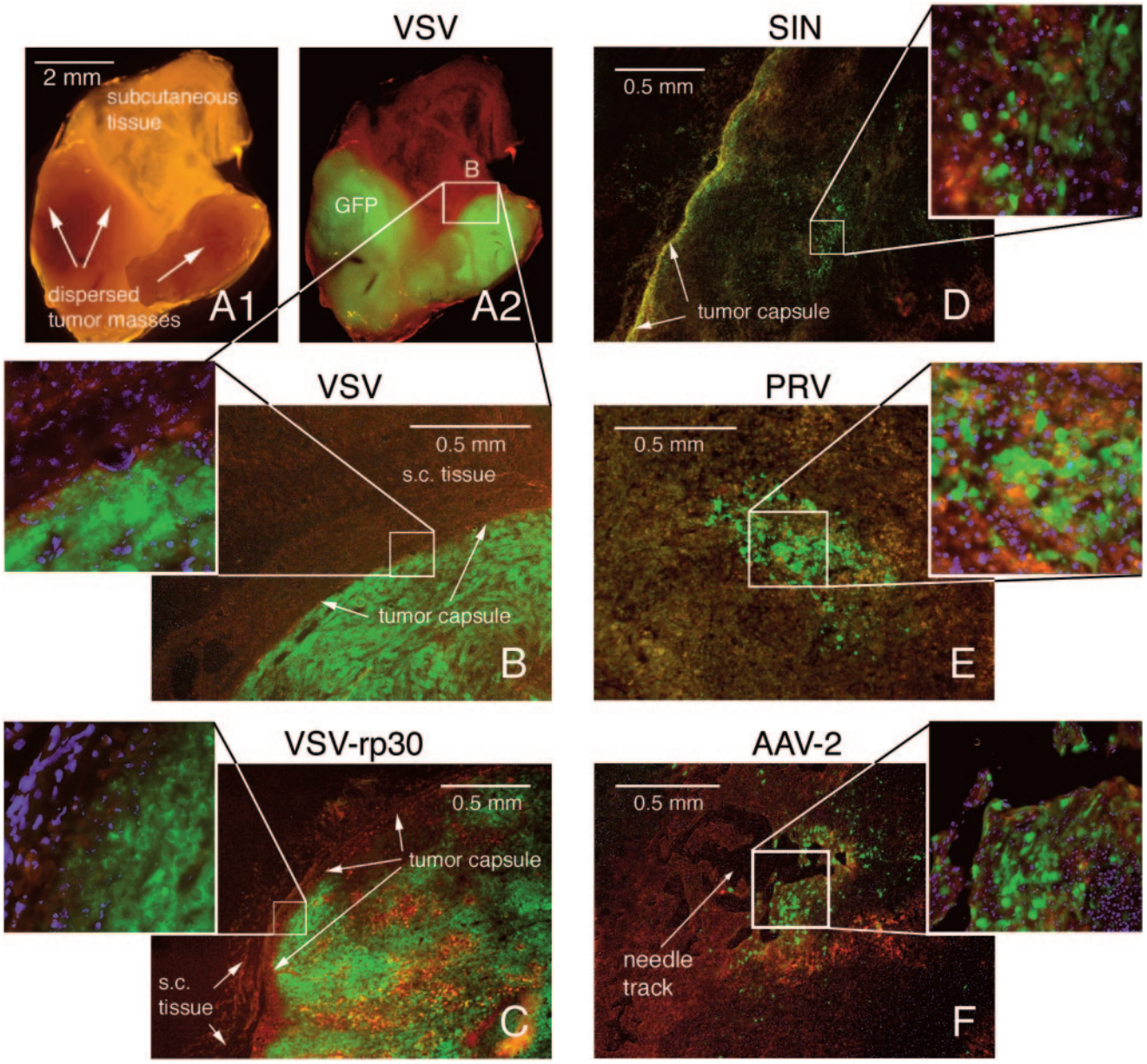

FIG. 8. Virus infection of glioblastoma xenografts in vivo. Images of tumor sections were taken using a multichannel fluorescence filter. Green indicates GFP expression, blue indicates nuclei stained with DAPI, and red-brown areas mark tissue background. (A1) Macroscopic aspect of a tissue block containing two small tumor masses that were remote from the original site of VSV injection. (A2) At 10 dpi, VSV selectively infected the small tumor masses. (B) Microscopic image of tumor mass shown in A. Note the demarcation at the tumor capsule. (C) At 10 days after intratumoral injection, VSV-rp30 has infected the whole tumor mass without crossing the tumor border (inset). (D) Intratumoral injection of SIN led to multiple widespread green islands and a distinct subcapsular green fluorescent band, indicating active viral spread. (E) Intratumoral injection with PRV at 10 dpi. The central area of the tumor is depicted. A similar spread was seen at 3 dpi. (F) Diffusion control with replication deficient AAV2. GFP expression was restricted to a 0.5-mm radius around the needle track.

Even 10 days after PRV inoculation, GFP expression was observed only in a central tumor area of ca. 1 mm^3 (Fig. 8E). The extent of GFP expression was not different from what we observed at 3 dpi, a finding indicative of relative little virus spread over time. Cellular fluorescence was bright, and morphological changes included loss of processes and cellular disintegration (inset in Fig. 8E). Green fluorescence was in large part associated with areas of cellular debris and granule-like figures, indicating cell death induction by PRV infection. Although cell lysis had occurred in infected areas, no substantial signs of further intratumoral spread of PRV were apparent.

GFP in infected cells could only be detected in a small area surrounding the needle track after AAV inoculation, with some single cells spread in a radius of about 0.5 to 1 mm, as shown in a typical section in Fig. 8F. Green cells exhibited a polymorphic appearance with preserved tumor cell processes (inset in Fig. 8F), indicating that the tumor integrity was not affected by AAV infection.

Together, the data gained from our in vivo proof-of-principle study substantiate the findings of the in vitro studies in general and of the replication assay in particular. As seen with the control AAV, replication deficiency limits the operating range of virus vectors to the immediate vicinity of the injection side. In contrast, both VSV and SIN penetrated through the tumor mass and, in the case of VSV, even reached the tumor border in a short period of time, without further invading the surrounding nontumor tissue at the time points studied.

DISCUSSION

There are currently no known medical or surgical approaches that constitute an effective treatment of glioblastoma, and most patients diagnosed with this type of brain tumor live less than a year. Since replication-competent viruses that could infect glioblastoma may be effective in the treatment of brain tumors, we tested the ability of nine different viruses to infect and kill selectively human glioblastoma in vitro and then used an in vivo model of solid human glioblastoma to test further the actions of viruses that were effective in vitro. A strain of glioblastoma-adapted VSV showed the greatest potential. SIN, MVMi, and MVMp also had some characteristics that showed promise. Human and mouse CMV, PRV, AAV, and SV40 were relatively ineffective.

Standardized test for viral effectiveness at targeting brain tumor cells. The strategy of using viruses to treat brain tumors has shown some promise for several viruses, including adenovirus, retrovirus, herpesvirus, poliovirus, vaccinia virus, measles virus, and H-1 parvovirus (11, 18, 21, 23, 42, 45, 46, 56, 61). However, the small number of viruses that have been utilized have generally been studied by different laboratories using multiple strategies on different cells and animal models, sometimes making it difficult to compare the potential of viral candidates. For this reason we used a series of eight tests, each addressing a different question relating to viral infection of tumor cells, including the expression of a reporter transgene, inhibition of glioblastoma mitosis, cytolytic action, genotype selectivity, glioblastoma selectivity compared to control cells, and in vivo substantiation of in vitro comparisons. This allowed a semiquantitative comparison of different viruses. An ideal virus for glioma virotherapy would selectively infect and kill glioblastoma cells and self-amplify its local action through viral replication. The behavior of the viruses with in vitro tests had strong predictive value relative to how the same virus performed in the in vivo model with solid glioblastoma tumors. The in vitro tests appeared reliable, and repetition of the same test months later generated the same quantitative results.

Use of replication-competent viruses. Although replication-incompetent viruses have been used with some success to deliver genes that kill tumor cells (35, 45), the range of oncolytic action is limited to the immediate site of application. Human trials have recently shown that the transfer efficiency of intratumorally injected replication-deficient retrovirus and adenovirus was small: in the range of 0.01 to 4% or 0.01 to 11%, respectively (44). Given this problem, the use of replication-competent viruses that have an affinity for a particular tumor type may ultimately prove more effective. To address the replication capacity of the viruses tested, we used a practical in vitro replication assay with small glass chips for isolated infection. The basic construct of transferring a very small number of infected cells onto a native tumor cell layer mimics the situation in situ, where only a small fraction of tumor cells get initially infected upon intratumoral injection. Not only was this test specific, as we have shown by the lack of viral spread of the replication-deficient AAV and recombinant SV40, it also served as a sensitive indicator, as can be seen by the strong correlation between the extent to which VSV, SIN, and PRV spread through the culture dish and the intratumoral spread observed in our in vivo solid tumor model.

Five of the viruses tested did replicate in glioblastoma cells. VSV and SIN progeny released from a small number of cells rapidly spread throughout the culture, ultimately killing all of the tumor cells. However, replication capability does not necessarily lead to self-amplification of the antitumor effect. Although PRV and both MVMi and MVMp showed definite and reproducible signs of viral spread, the effect on the tumor cells was limited. Confirming this observation, the area of intratumoral spread of PRV in an in vivo model was small, with little sign of spread at the longer time of action.

Virus generalization and specificity for different glioblastoma lineages. To accommodate the heterogeneity of glioblastomas in our evaluation of viruses, we compared the oncolytic potential of the viruses in two different types of glioblastoma: U-87 MG and M059J. U-87 MG cells are hypodiploid, with a number of mutations that commonly occur in glioblastoma cells, i.e., multiple mutations in PTEN, deletions in p16, p14, and alpha interferon, production of transforming growth factor, and overexpression of EGFR and PDGFR. In contrast, p53 is wild type in these tumor cells (1, 24, 37, 39). M059J cells, on the other hand, are nearly pentaploid, with frequent aberrations on chromosome 8, are homozygous for a single point mutation in the TP53 gene, and are defective in the DNA-PK-mediated repair of DNA damage (3, 4). Although two cell lines do not cover the full extent of the genotype anomalies found in glioblastoma, they do serve as an example for testing whether a virus action has a more universal or restricted cell type affinity.

VSV rapidly infected and killed both cell lines, indicating a likely general targeting of glioma cells. In contrast to VSV, three of the viruses showed preferences for a single glioblastoma genotype: SIN for U-87 MG and MVMi and MVMp for M059J. In contrast to SIN, MVM showed a much stronger effect on M059J. The cytotoxic effect of MVM has been ascribed to the viral NS-1 protein and may be particularly effective in cells lacking functional p53 (41). The mutation of p53 in M059J cells (3) might provide a possible explanation for the MVM cell preference.

Tumor cell specificity of viral infection and cytolysis. The initial set of experiments included nine viruses and addressed their ability to infect and kill human glioblastoma cells. Of the original collection, five viruses had potential oncolytic profiles. An equally important parameter for the evaluation of viral candidates is defined by the oncospecificity. The tumor-restricted replication and lysis is critical for any potential viral treatment, particularly in such a sensitive area as the brain. The lack of viral affinity for neurons is important, but primary cultures of human adult neurons are not readily available. Therefore, finding an appropriate in vitro control for human nonmalignant brain tissue remains a challenge.

SIN and the two MVM strains did not significantly infect human fibroblasts while selectively infecting and destroying cocultured U-87 MG glioblastoma cells. The underlying mechanisms defining SIN selectivity might lie at the level of its interactions at the cell surface (25). On the other hand, MVM is known to exhibit an inherent oncotropism at the intracellular level, since the initiation of the virus life cycle depends on host cell factors provided by actively dividing cells in S phase and the transcriptional makeup of the tumor cell (13).

VSV showed relative selectivity for glioblastoma cells. After initial infection, GFP expression and cytotoxic effects were primarily evident in tumor cells, whereas nontumor fibroblasts were spared. However, the accumulation of viral progeny released from infected U-87 MG cells might have contributed to the latent development of GFP and cell death among the control cells. The selective potential of VSV was enhanced when we compared the action of the passage-adapted VSV-rp30 with the original VSV in a modified coculture assay. Here, VSV-rp30 rapidly killed U-87 MG cells within a day without infecting cocultured fibroblasts, which remained intact even through a 1-week observation period. Since mechanisms for VSV attachment and cell entry do not appear to be cell selective (47), the selectivity of VSV infection is most likely controlled intracellularly. The cellular interferon system restrains VSV replication and spread in normal cells; in contrast, the defective nature of interferon protection in numerous tumors might enhance the oncoselectivity of VSV (53).

In contrast, PRV-infected and killed human fibroblasts with greater efficiency than glioblastoma cells, reducing its potential for focused oncolytic actions.

Relative efficiency of different viruses in glioblastoma cells. Of the nine viruses used, four were relatively ineffective. As expected, the replication-incompetent AAV used as a control infected many cells but, as the tumor cells divided, AAV was unable to infect successive generations of tumor cells; injections of AAV into a solid tumor in vivo showed infection only at the site of injection, suggesting that even carrying a toxic gene, this or other replication-deficient viruses could at best only kill tumor cells in the immediate vicinity of the injection. Similarly, mouse CMV infected a minority of tumor cells but, in the absence of replication in human cells, would not be effective. Although some reports have suggested that human CMV might show some affinity for astrocytes (32), the virus was relatively ineffective at replicating on human glioblastoma. Both a recombinant SV40 lacking large T and wild-type SV40, which has also been reported to have some affinity for brain tumors (62), showed only low levels of infection and little cytolytic action.

PRV at high concentrations did infect and kill both types of glioblastoma cells, but at low concentrations it was relatively ineffective at infecting the rapidly dividing tumor cells. Similarly, PRV showed only modest infection of solid tumors in vivo, with relatively little spread within the tumor. Serial passage adaptation might enhance the ability of PRV to infect glioblastoma but, since PRV can have lethal consequences after retrograde transport into the brain of rodents and other mammals, the health risk to humans that normally are not affected negatively by PRV might increase substantially. PRV exhibited a high affinity for normal human fibroblasts, underlining the lack of specificity for glioblastoma. PRV has been reported to be more effective at killing rodent-derived tumors than human-derived tumors from several organs (9).

Both MVM strains showed considerable tumor-suppressive action at high virus concentrations. However, they showed only a mild effect at low virus concentrations and, although they replicated in glioblastoma cells, the rapid growth of the tumor cell population outpaced the virus replication. Autonomous parvoviruses share the desired feature of dependence on host cell factors provided during the S phase of cell division, preventing MVM replication in postmitotic neurons. An important additional consideration for a potential application of MVM against malignant brain tumors is its relative dependence on defects in the p53 pathway, a frequent mutation in malignancies of astrocytic lineage. A previous report found that MVMp replicated to a lower extent, and with less cell killing, in U-87 MG glioma cells than it does in U373 glioma cells (48), a line that, such as M059J, appears to have a p53 mutation (1, 24). Taken together, MVM has an interesting profile combining inherent oncotropism and moderate oncolytic efficiency with a high potential safety for postmitotic cells. Attempts to enhance the tumor-suppressive effect of MVM have been made by inserting immunostimulatory or cell suicide genes into MVM-based vectors (13, 16) with promising outcomes; however, these vectors were replication incompetent and so might have only local effectiveness.

The efficient oncolytic profile that SIN showed against U-87 MG cells in vitro and in vivo combined with its lack of infection of nonmalignant control cells renders SIN a promising candidate for future experiments toward refining its potential for treating brain tumors. However, the lack of a general antiglioma spectrum has to be taken into account and might limit the number of tumor cells being targeted. Systemically applied SIN can target non-CNS peripheral tumors and induce apoptosis therein (57), but this has not been examined in detail in the brain. SIN exhibits a direct oncolytic effect by inducing apoptosis upon cell entry, and natural killer cells may enhance the tumor suppressive effect. Some strains of SIN can be neurovirulent (20, 31), whereas the less pathogenic strain, AR339, used in our study appears to be less neurotoxic.

VSV demonstrated the strongest tumor-suppressive action of all of the viruses examined in the present study. The combination of rapid infection, cell lysis, and replication-based self-amplification and spread show promise for this virus in targeting and killing glioblastomas. A variant we produced by serial passage on glioblastoma cells, VSV-rp30, showed an enhanced preference for glioblastoma over control cells, an increased cytolytic activity on brain tumor cells, and also worked well to spread through solid glioblastoma in an in vivo model. The increased antiglioma profile was not limited to the cell line on which VSV-rp30 was originally passaged. The general higher affinity for numerous glioblastoma types with distinct mutation patterns and growth characteristics appears to be especially valuable considering the heterogeneous nature of these tumors. Work on other tumor cell types has shown that VSV has oncolytic potential. Tumor selectivity may be enhanced by mutations in the VSV-M protein that can block antiviral interferon responses in normal cells that are initiated by double-stranded RNA-dependent protein kinase (5, 53). The mutant VSV-rp30 may hypothetically have a mutation in the M protein, which would reduce its capacity to kill normal

cells. The oncoselectivity of VSV is not restricted to fast-dividing cells. It appears able to target both mitotic and quiescent glioblastoma cells; the latter often escape current chemotherapy or radiation therapy treatments. Other studies have shown that VSV can be effective and selective at killing several peripheral tumor cell types; here, we generated a new variant strain, VSV-rp30, that is effective at selectively infecting and killing glioblastoma cells. Tumor cell adaptation may have considerable potential for targeting a rather heterogeneous malignancy such as glioblastoma.

Given that current treatments of glioblastoma are relatively ineffective, the use of replication-competent viruses merits consideration. The greatest concern relates to the possibility of viral spread and damage to normal brain cells around a tumor. This is particularly important in the CNS, since neurons show little postnatal replication. Viral attack of neurons would be less of a problem for MVM since it would not replicate in postmitotic cells, but is a concern for SIN, VSV, and particularly PRV. Future work on potential mechanisms for controlling further viral spread to normal cells, including astrocytes and neurons, is needed. In this regard, the addition to the virus genome of suicide genes such as those coding for thymidine kinase or cytosine deaminase may limit the spread of infection into normal brain tissue by eliminating infected cells. Other possibilities for harnessing oncolytic viruses include the use of conditional promoters upon which viral replication is dependent, mutation of viral genes such as the M protein in VSV that suppress immune responses in normal cells, insertion of an inducible small interfering RNA in appropriate viral genomes to block viral replication, or enhancement of the immune system to target virus-infected cells.

ACKNOWLEDGMENTS

We thank Joseph Piepmeier, Joachim Baehring, and Lei Li for encouragement, suggestions, and advice and Y. Yang and V. Rougulin for technical facilitation.

Grant support was provided by the NIH (AI/NS48854, NS34887, and NS37788) and the NCI (CA29303).

REFERENCES

1. **Ali-Osman, F.** 1999. Brain tumors, p. 167–184. *In* J. R. W. Masters and B. Palson (ed.), Human cell culture, vol. 2. Kluwer Academic Publishers, New York, N.Y.
2. **American Cancer Society Surveillance Research.** 2002. Cancer facts and figures 2002. American Cancer Society, Inc., Atlanta, Ga.
3. **Anderson, C. W., and M. J. Allalunis-Turner.** 2000. Human TP53 from the malignant glioma-derived cell lines M059J and M059K has a cancer-associated mutation in exon 8. Radiat. Res. **154:**473–476.
4. **Anderson, C. W., J. J. Dunn, P. I. Freimuth, A. M. Galloway, and M. J. Allalunis-Turner.** 2001. Frameshift mutation in PRKDC, the gene for DNA-PKcs, in the DNA repair-defective, human, glioma-derived cell line M059J. Radiat. Res. **156:**2–9.
5. **Balachandran, S., and G. N. Barber.** 2000. Vesicular stomatitis virus (VSV) therapy of tumors. IUBMB Life **50:**135–138.
6. **Balachandran, S., M. Porosnicu, and G. N. Barber.** 2001. Oncolytic activity of vesicular stomatitis virus is effective against tumors exhibiting aberrant p53, Ras, or myc function and involves the induction of apoptosis. J. Virol. **75:**3474–3479.
7. **Ball-Goodrich, L. J., and P. Tattersall.** 1992. Two amino acid substitutions within the capsid are coordinately required for acquisition of fibrotropism by the lymphotropic strain of minute virus of mice. J. Virol. **66:**3415–3423.
8. **Bantel-Schaal, U.** 1990. Adeno-associated parvoviruses inhibit growth of cells derived from malignant human tumors. Int. J. Cancer **45:**190–194.
9. **Boldogkoi, Z., A. Bratincsak, and I. Fodor.** 2002. Evaluation of pseudorabies virus as a gene transfer vector and an oncolytic agent for human tumor cells. Anticancer Res. **22:**2153–2159.
10. **Card, J. P., and L. W. Enquist.** 1995. Neurovirulence of pseudorabies virus. Crit. Rev. Neurobiol. **9:**137–162.
11. **Chiocca, E. A., M. Aghi, and G. Fulci.** 2003. Viral therapy for glioblastoma. Cancer J. **9:**167–179.
12. **Clark, K. R., X. Liu, J. P. McGrath, and P. R. Johnson.** 1999. Highly purified recombinant adeno-associated virus vectors are biologically active and free of detectable helper and wild-type viruses. Hum. Gene Ther. **10:**1031–1039.
13. **Cornelis, J. J., N. Salome, C. Dinsart, and J. Rommelaere.** 2004. Vectors based on autonomous parvoviruses: novel tools to treat cancer? J. Gene Med. **6**(Suppl. 1)**:**S193–S202.
14. **Dalton, K. P., and J. K. Rose.** 2001. Vesicular stomatitis virus glycoprotein containing the entire green fluorescent protein on its cytoplasmic domain is incorporated efficiently into virus particles. Virology **279:**414–421.
15. **Drake, J. W., and J. J. Holland.** 1999. Mutation rates among RNA viruses. Proc. Natl. Acad. Sci. USA **96:**13910–13913.
16. **Dupont, F., B. Avalosse, A. Karim, N. Mine, M. Bosseler, A. Maron, A. V. Van den Broeke, G. E. Ghanem, A. Burny, and M. Zeicher.** 2000. Tumor-selective gene transduction and cell killing with an oncotropic autonomous parvovirus-based vector. Gene Ther. **7:**790–796.
17. **Gardiner, E. M., and P. Tattersall.** 1988. Evidence that developmentally regulated control of gene expression by a parvoviral allotropic determinant is particle mediated. J. Virol. **62:**1713–1722.
18. **Germano, I. M., J. Fable, S. H. Gultekin, and A. Silvers.** 2003. Adenovirus/herpes simplex-thymidine kinase/ganciclovir complex: preliminary results of a phase I trial in patients with recurrent malignant gliomas. J. Neurooncol. **65:**279–289.
19. **Griffin, D. E.** 2001. Alphaviruses, p. 917–962. *In* D. M. Knipe and P. M. Howley (ed.), Fields virology, 4th ed. Lippincott-Raven Publishers, Philadelphia, Pa.
20. **Griffin, D. E., and J. M. Hardwick.** 1997. Regulators of apoptosis on the road to persistent alphavirus infection. Annu. Rev. Microbiol. **51:**565–592.
21. **Gromeier, M., S. Lachmann, M. R. Rosenfeld, P. H. Gutin, and E. Wimmer.** 2000. Intergeneric poliovirus recombinants for the treatment of malignant glioma. Proc. Natl. Acad. Sci. USA **97:**6803–6808.
22. **Hardwick, J. M., and B. Levine.** 2000. Sindbis virus vector system for functional analysis of apoptosis regulators. Methods Enzymol. **322:**492–508.
23. **Herrero, Y. C. M., J. J. Cornelis, C. Herold-Mende, J. Rommelaere, J. R. Schlehofer, and K. Geletneky.** 2004. Parvovirus H-1 infection of human glioma cells leads to complete viral replication and efficient cell killing. Int. J. Cancer **109:**76–84.
24. **Ishii, N., D. Maier, A. Merlo, M. Tada, Y. Sawamura, A. C. Diserens, and E. G. Van Meir.** 1999. Frequent co-alterations of TP53, p16/CDKN2A, p14ARF, PTEN tumor suppressor genes in human glioma cell lines. Brain Pathol. **9:**469–479.
25. **Jan, J. T., S. Chatterjee, and D. E. Griffin.** 2000. Sindbis virus entry into cells triggers apoptosis by activating sphingomyelinase, leading to the release of ceramide. J. Virol. **74:**6425–6432.
26. **Jarvis, M. A., C. E. Wang, H. L. Meyers, P. P. Smith, C. L. Corless, G. J. Henderson, J. Vieira, W. J. Britt, and J. A. Nelson.** 1999. Human cytomegalovirus infection of caco-2 cells occurs at the basolateral membrane and is differentiation state dependent. J. Virol. **73:**4552–4560.
27. **Jasani, B., A. Cristaudo, S. A. Emri, A. F. Gazdar, A. Gibbs, B. Krynska, C. Miller, L. Mutti, C. Radu, M. Tognon, and A. Procopio.** 2001. Association of SV40 with human tumours. Semin. Cancer Biol. **11:**49–61.
28. **Lawson, N. D., E. A. Stillman, M. A. Whitt, and J. K. Rose.** 1995. Recombinant vesicular stomatitis viruses from DNA. Proc. Natl. Acad. Sci. USA **92:**4477–4481.
29. **Legrand, C., J. Rommelaere, and P. Caillet-Fauquet.** 1993. MVM(p) NS-2 protein expression is required with NS-1 for maximal cytotoxicity in human transformed cells. Virology **195:**149–155.
30. **Levin, V. A., S. A. Leibel, and P. H. Gutin.** 1997. Neoplasms of the central nervous system, p. 2022–2082. *In* V. T. DeVitra, Jr., S. Hellman, and S. A. Rosenberg (ed.), Cancer principles and practice of oncology, 5th ed. Lippincott-Raven, Philadelphia, Pa.
31. **Lewis, J., S. L. Wesselingh, D. E. Griffin, and J. M. Hardwick.** 1996. Alphavirus-induced apoptosis in mouse brains correlates with neurovirulence. J. Virol. **70:**1828–1835.
32. **Lokensgard, J. R., M. C. Cheeran, G. Gekker, S. Hu, C. C. Chao, and P. K. Peterson.** 1999. Human cytomegalovirus replication and modulation of apoptosis in astrocytes. J. Hum. Virol. **2:**91–101.
33. **Ma, H. I., S. Z. Lin, Y. H. Chiang, J. Li, S. L. Chen, Y. P. Tsao, and X. Xiao.** 2002. Intratumoral gene therapy of malignant brain tumor in a rat model with angiostatin delivered by adeno-associated viral (AAV) vector. Gene Ther. **9:**2–11.
34. **Maxwell, I. H., K. L. Terrell, and F. Maxwell.** 2002. Autonomous parvovirus vectors. Methods **28:**168–181.
35. **Mizuno, M., J. Yoshida, P. Colosi, and G. Kurtzman.** 1998. Adeno-associated virus vector containing the herpes simplex virus thymidine kinase gene causes complete regression of intracerebrally implanted human gliomas in mice, in conjunction with ganciclovir administration. Jpn J. Cancer Res. **89:**76–80.
36. **Mocarski, E. S., and C. T. Courcelle.** 2001. Cytomegaloviruses and their replication, p. 2629–2673. *In* D. M. Knipe and P. M. Howley (ed.), Fields virology, 4th ed. Lippincott-Raven Publishers, Philadelphia, Pa.

37. **Mohapatra, G., D. H. Kim, and B. G. Feuerstein.** 1995. Detection of multiple gains and losses of genetic material in ten glioma cell lines by comparative genomic hybridization. Genes Chromosomes Cancer **13:**86–93.
38. **Naeger, L. K., E. C. Goodwin, E. S. Hwang, R. A. DeFilippis, H. Zhang, and D. DiMaio.** 1999. Bovine papillomavirus E2 protein activates a complex growth-inhibitory program in p53-negative HT-3 cervical carcinoma cells that includes repression of cyclin A and cdc25A phosphatase genes and accumulation of hypophosphorylated retinoblastoma protein. Cell Growth Differ. **10:**413–422.
39. **Nister, M., T. A. Libermann, C. Betsholtz, M. Pettersson, L. Claesson-Welsh, C. H. Heldin, J. Schlessinger, and B. Westermark.** 1988. Expression of messenger RNAs for platelet-derived growth factor and transforming growth factor-alpha and their receptors in human malignant glioma cell lines. Cancer Res. **48:**3910–3918.
40. **Obuchi, M., M. Fernandez, and G. N. Barber.** 2003. Development of recombinant vesicular stomatitis viruses that exploit defects in host defense to augment specific oncolytic activity. J. Virol. **77:**8843–8856.
41. **Op De Beeck, A., J. Sobczak-Thepot, H. Sirma, F. Bourgain, C. Brechot, and P. Caillet-Fauquet.** 2001. NS1- and minute virus of mice-induced cell cycle arrest: involvement of p53 and $p21^{cip1}$. J. Virol. **75:**11071–11078.
42. **Phuong, L. K., C. Allen, K. W. Peng, C. Giannini, S. Greiner, C. J. TenEyck, P. K. Mishra, S. I. Macura, S. J. Russell, and E. C. Galanis.** 2003. Use of a vaccine strain of measles virus genetically engineered to produce carcinoembryonic antigen as a novel therapeutic agent against glioblastoma multiforme. Cancer Res. **63:**2462–2469.
43. **Prieto, J., J. Solera, and E. Tabares.** 2002. Development of new expression vector based on pseudorabies virus amplicons: application to human insulin expression. Virus Res. **89:**123–129.
44. **Puumalainen, A. M., M. Vapalahti, R. S. Agrawal, M. Kossila, J. Laukkanen, P. Lehtolainen, H. Viita, L. Paljarvi, R. Vanninen, and S. Yla-Herttuala.** 1998. Beta-galactosidase gene transfer to human malignant glioma in vivo using replication-deficient retroviruses and adenoviruses. Hum. Gene Ther. **9:**1769–1774.
45. **Rainov, N. G., and H. Ren.** 2003. Clinical trials with retrovirus mediated gene therapy—what have we learned? J. Neurooncol. **65:**227–236.
46. **Rainov, N. G., and H. Ren.** 2003. Gene therapy for human malignant brain tumors. Cancer J. **9:**180–188.
47. **Rose, J. K., and M. A. Whitt.** 2001. *Rhabdoviridae*: the viruses and their replication, p. 1221–1244. *In* D. M. Knipe and P. M. Howley (ed.), Fields virology, 4th ed. Lippincott-Raven Publishers, Philadelphia, Pa.
48. **Rubio, M. P., S. Guerra, and J. M. Almendral.** 2001. Genome replication and postencapsidation functions mapping to the nonstructural gene restrict the host range of a murine parvovirus in human cells. J. Virol. **75:**11573–11582.
49. **Russell, S. J., A. Brandenburger, C. L. Flemming, M. K. Collins, and J. Rommelaere.** 1992. Transformation-dependent expression of interleukin genes delivered by a recombinant parvovirus. J. Virol. **66:**2821–2828.
50. **Schlehofer, J. R.** 1994. The tumor suppressive properties of adeno-associated viruses. Mutat. Res. **305:**303–313.
51. **Shaughnessy, E., D. Lu, S. Chatterjee, and K. K. Wong.** 1996. Parvoviral vectors for the gene therapy of cancer. Semin. Oncol. **23:**159–171.
52. **Smith, B. N., B. W. Banfield, C. A. Smeraski, C. L. Wilcox, F. E. Dudek, L. W. Enquist, and G. E. Pickard.** 2000. Pseudorabies virus expressing enhanced green fluorescent protein: a tool for in vitro electrophysiological analysis of transsynaptically labeled neurons in identified central nervous system circuits. Proc. Natl. Acad. Sci. USA **97:**9264–9269.
53. **Stojdl, D. F., B. Lichty, S. Knowles, R. Marius, H. Atkins, N. Sonenberg, and J. C. Bell.** 2000. Exploiting tumor-specific defects in the interferon pathway with a previously unknown oncolytic virus. Nat. Med. **6:**821–825.
54. **Stojdl, D. F., B. D. Lichty, B. R. tenOever, J. M. Paterson, A. T. Power, S. Knowles, R. Marius, J. Reynard, L. Poliquin, H. Atkins, E. G. Brown, R. K. Durbin, J. E. Durbin, J. Hiscott, and J. C. Bell.** 2003. VSV strains with defects in their ability to shutdown innate immunity are potent systemic anti-cancer agents. Cancer Cell **4:**263–275.
55. **Tattersall, P., and J. Bratton.** 1983. Reciprocal productive and restrictive virus-cell interactions of immunosuppressive and prototype strains of minute virus of mice. J. Virol. **46:**944–955.
56. **Timiryasova, T. M., J. Li, B. Chen, D. Chong, W. H. Langridge, D. S. Gridley, and I. Fodor.** 1999. Antitumor effect of vaccinia virus in glioma model. Oncol. Res. **11:**133–144.
57. **Tseng, J. C., B. Levin, A. Hurtado, H. Yee, I. Perez de Castro, M. Jimenez, P. Shamamian, R. Jin, R. P. Novick, A. Pellicer, and D. Meruelo.** 2004. Systemic tumor targeting and killing by Sindbis viral vectors. Nat. Biotechnol. **22:**70–77.
58. **van den Pol, A. N., K. P. Dalton, and J. K. Rose.** 2002. Relative neurotropism of a recombinant rhabdovirus expressing a green fluorescent envelope glycoprotein. J. Virol. **76:**1309–1327.
59. **van den Pol, A. N., E. Mocarski, N. Saederup, J. Vieira, and T. J. Meier.** 1999. Cytomegalovirus cell tropism, replication, and gene transfer in brain. J. Neurosci. **19:**10948–10965.
60. **Van den Pol, A. N., J. Vieira, D. D. Spencer, and J. G. Santarelli.** 2000. Mouse cytomegalovirus in developing brain tissue: analysis of 11 species with GFP-expressing recombinant virus. J. Comp. Neurol. **427:**559–580.
61. **Vecil, G. G., and F. F. Lang.** 2003. Clinical trials of adenoviruses in brain tumors: a review of Ad-p53 and oncolytic adenoviruses. J. Neurooncol. **65:**237–246.
62. **Vilchez, R. A., and J. S. Butel.** 2003. SV40 in human brain cancers and non-Hodgkin's lymphoma. Oncogene **22:**5164–5172.
63. **Wang, K. S., R. J. Kuhn, E. G. Strauss, S. Ou, and J. H. Strauss.** 1992. High-affinity laminin receptor is a receptor for Sindbis virus in mammalian cells. J. Virol. **66:**4992–5001.
64. **Wrensch, M., Y. Minn, T. Chew, M. Bondy, and M. S. Berger.** 2002. Epidemiology of primary brain tumors: current concepts and review of the literature. Neuro-oncology **4:**278–299.
65. **Yoshida, J., M. Mizuno, N. Nakahara, and P. Colosi.** 2002. Antitumor effect of an adeno-associated virus vector containing the human interferon-beta gene on experimental intracranial human glioma. Jpn. J. Cancer Res. **93:** 223–228.
66. **Zeicher, M., P. Spegelaere, M. Horth, D. Gancberg, A. Karim, and F. Dupont.** 2003. Oncoselective parvoviral vector-mediated gene therapy of cancer. Oncol. Res. **13:**437–444.
67. **Zrachia, A., M. Dobroslav, M. Blass, G. Kazimirsky, I. Kronfeld, P. M. Blumberg, D. Kobiler, S. Lustig, and C. Brodie.** 2002. Infection of glioma cells with Sindbis virus induces selective activation and tyrosine phosphorylation of protein kinase C delta. Implications for Sindbis virus-induced apoptosis. J. Biol. Chem. **277:**23693–23701.